

AD-755 213

HIGH POWER ALKALI VAPOR LAMPS

Lowell Noble, et al

ILC Technology, Incorporated

Prepared for:

Advanced Research Projects Agency  
Office of Naval Research

January 1973

DISTRIBUTED BY:

**NTIS**

National Technical Information Service  
U. S. DEPARTMENT OF COMMERCE  
5285 Port Royal Road, Springfield Va. 22151



AD 755213



Reproduced by  
**NATIONAL TECHNICAL  
INFORMATION SERVICE**  
U S Department of Commerce  
Springfield VA 22151

77



HIGH POWER ALKALI VAPOR LAMPS  
FINAL REPORT



UNCLASSIFIED

2

Security Classification

## DOCUMENT CONTROL DATA - R &amp; D

(Security classification of title, body of abstract and indexing annotation must be entered when the overall report is classified.)

1. ORIGINATING ACTIVITY (Corporate author) ILC Technology, Inc. 164 Commercial Street Sunnyvale, California 94086		2a. REPORT SECURITY CLASSIFICATION Unclassified	
3. REPORT TITLE High Power Alkali Vapor Lamps		2b. GROUP	
4. DESCRIPTIVE NOTES (Type of report and inclusive dates) Final Report			
5. AUTHOR(S) (First name, middle initial, last name) Lowell Noble and Carl Kretschmer			
6. REPORT DATE March 1971 - September 1972		7a. TOTAL NO. OF PAGES 77	7b. NO. OF RLFS 13
8a. CONTRACT OR GRANT NO. N00014-71-C-0183		9a. ORIGINATOR'S REPORT NUMBER(S)	
b. PROJECT NO.		9b. OTHER REPORT NO(S) (Any other numbers that may be assigned this report) ARPA Order No. 306	
c.			
d.			
10. DISTRIBUTION STATEMENT			
11. SUPPLEMENTARY NOTES		12. SPONSORING MILITARY ACTIVITY Office of Naval Research Physical Sciences Division Arlington, Virginia 22217	
13. ABSTRACT The objective of this contract was to develop and deliver prototype 6.4 kW (input power) alkali vapor lamps that would emit 2 kW of output radiation in the major pumping bands of Nd:YAG laser material. The lamps were to be 8 inches long and 18 mm or less in outside diameter, and were to provide an operational lifetime of 100 hours or more. (1) Lamps with transparent sapphire envelopes of 14.5 mm bore diameter were built and operated successfully at input powers of up to 800 W per inch of arc length, corresponding to the design goal of 6.4 kW for an 8 inch arc length. Initial difficulties in controlling the alkali metal vapor pressure to provide optimal spectral matching to the absorption bands of the laser material were overcome by design changes in the liquid metal reservoir. When optimally matched, these lamps were more efficient in producing radiation in the pump bands of Nd:YAG than krypton arc lamps of the same length and input power. However, the krypton arc lamps had a smaller arc diameter and provided higher brightness in the useful pump bands. Tests on smaller bore lamps showed that the addition of excesses of argon or mercury to the standard K-Rb fill does not produce significant improvement in spectral matching or efficiency. Spectrophotometric and calorimetric equipment developed for the program is described, and a theoretical derivation of the relations between bore diameter, input power, and efficiency is presented. At the end of the program, four lamps with 14.5 mm bore and 8 inch arc length (to match the length of a specified laser) were delivered. The lamps were enclosed in quartz envelopes of 18 mm outside diameter, matching the diameter requirement of that laser.			

DD FORM 1473  
1 NOV 68REPLACES DD FORM 1473, 1 JAN 64, WHICH IS  
OBSOLETE FOR ARMY USE.

UNCLASSIFIED

Security Classification



UNCLASSIFIED

Security Classification

3

14.	KEY WORDS	LINK A		LINK B		LINK C	
		ROLE	WT	ROLE	WT	ROLE	WT
	Optical Pumps CW Lamps Alkali Metal Lamps Potassium Lamps Lasers Laser Pumps Radiative Transfer						

UNCLASSIFIED

Security Classification





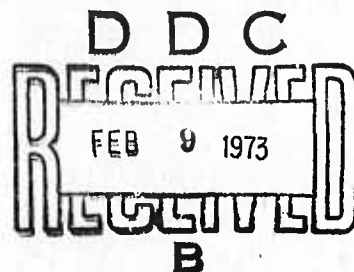
ILC Technology

FINAL REPORT

4

JANUARY 1973

HIGH POWER ALKALI VAPOR LAMPS  
MARCH 1971 - SEPTEMBER 1972  
R-ILC-72-31




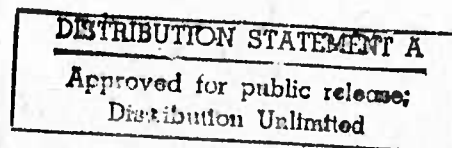
By: Mr. Lowell Noble  
and  
Dr. Carl Kretschmer

Prepared for: Office of Naval Research  
Physical Sciences Division  
Arlington, Virginia 22217

Contract No.: N00014-71-C-0183

APPROVED:

  
G. Sorenson, President



This research was supported by the Advanced  
Research Projects Agency of the Department of  
Defense and was monitored by ONR under  
Contract No. N00014-71-C-0183

The views and conclusions contained in this document are those of the authors  
and should not be interpreted as necessarily representing the official policies,  
either expressed or implied, of the Advanced Research Projects Agency or the  
U.S. Government.

164 Commercial Street □ Sunnyvale, California 94086 □ Phone 408/738-2944



ILC Technology, Inc.

January 1973

HIGH POWER ALKALI VAPOR LAMPS  
FINAL REPORT

For:

OFFICE OF NAVAL RESEARCH  
CONTRACT NO. N00014-71-C-0183  
MARCH 1971 - SEPTEMBER 1972  
AMOUNT OF CONTRACT: \$75,000

Principal Investigator:

Mr. Lowell Noble  
ILC Technology, Inc.  
164 Commercial Street  
Sunnyvale, Calif. 94086  
(408) 738-2944

Scientific Officer:

Director, Physics Branch  
Physical Sciences Division  
Office of Naval Research  
Department of the Navy  
Arlington, Virginia 22217

Sponsored By:

ADVANCED RESEARCH PROJECTS AGENCY  
ARPA Order No. 306  
Program Code No. S0507A

Prepared By:

ILC Technology, Inc.  
Sunnyvale, California



## FOREWORD

This work was carried out by the Engineering Division of ILC Technology, Inc., which is under the direction of Dr. I. Reed. The Technical Monitor of the program was Dr. Fred Quell, Office of Naval Research.

The Principal Investigator was Mr. I. Noble. He was assisted by Dr. C. E. Kretschmer. Mr. R. Maynard performed the experimental measurements and data reduction. Mr. J. Gaspar was responsible for alkali vapor lamp fabrication.

Work on this contract began on 5 March 1971 and ended on 29 September 1972.



## TABLE OF CONTENTS

	<u>Page No.</u>
ABSTRACT	
FOREWORD	
LIST OF ILLUSTRATIONS	
SUMMARY	
1.0 INTRODUCTION AND OBJECTIVE	1
2.0 BACKGROUND	1
3.0 EXPERIMENTAL APPROACH	4
4.0 EXPERIMENTAL PROCEDURE	5
4.1 Lamp Construction	5
4.1.1 Alkali Metal Vapor Lamps	5
4.1.2 Krypton Lamps	7
4.2 Spectral Measurements	8
4.2.1 Absolute Spectral Irradiance Measurements	8
4.2.2 Relative "Effective" Irradiance Measurements	9
4.2.3 Relative "Effective" Radiance Measurements	11
4.3 Calorimetric Measurements	11
4.4 Arc Diameter Measurements	12
5.0 EXPERIMENTAL RESULTS	12
5.1 Results for 5 mm and 6.3 mm bore, 3 Inch Arc Length Alkali Metal Vapor Lamps	12



## Table of Contents - Continued

	<u>Page No.</u>
5.2 Results for 14.5 mm Bore, 3 Inch arc Length, K-Rb 50 Torr Argon Filled Alkali Metal Vapor Lamp	15
5.3 Results for 4, 6, and 10 mm Bore, 3 Inch Arc Length, 3 Atmosphere Filled Krypton Arc Lamps	19
6.0 DISCUSSION	20
6.1 Performance of Large-Bore Alkali Vapor Arc Lamps in Pumping Nd:YAG Laser Material	20
6.2 Scaling Relations for Resonance Radiation- Dominated Arcs	20
6.3 Control of Vapor Pressure	24
6.4 Effect of Increased Argon Pressure	24
6.5 Effect of Adding Mercury	25
6.6 Beryllium Oxide Envelope Lamps	25
6.7 Radiative Efficiency of Krypton Arc Lamps	25
7.0 CONCLUSIONS	26
LITERATURE CITED	
APPENDIX I	



## LIST OF ILLUSTRATIONS

- FIGURE 1      ALKALI METAL LAMP CONFIGURATIONS (4258)
- FIGURE 2      LASER DATA FOR ALKALI VAPOR LAMPS AND A KRYPTON  
ARC LAMP (1059)
- FIGURE 3      EXCITATION SPECTRA FOR Nd:YAG (1001)
- FIGURE 4      SPECTRUM FROM ALKALI VAPOR LAMP AT OPTIMUM  
PRESSURE (1055)
- FIGURE 5      POTASSIUM EMISSION SPECTRUM AS A FUNCTION OF  
PRESSURE (1036)
- FIGURE 6      ALKALI METAL LAMP, 14.5 mm BORE DIAMETER (4481)
- FIGURE 7      MOUNTING FIXTURE FOR CONTROLLING RESERVOIR  
TEMPERATURE OF ALKALI VAPOR ARC LAMP (4482)
- FIGURE 8      KRYPTON ARC LAMP WITH EXTERNALLY WATER COOLED  
ELECTRODES (4484)
- FIGURE 9      KRYPTON ARC LAMP WITH INTERNALLY WATER COOLED  
ELECTRODES (4484)
- FIGURE 10     KRYPTON ARC LAMPS WITH INTERNALLY WATER COOLED  
ELECTRODES. 10 mm BORE DIAMETER, 8 kW AND 20 kW  
(4485)
- FIGURE 11     SCHEMATIC DIAGRAM OF EQUIPMENT FOR RECORDING  
LAMP SPECTRA (4018)
- FIGURE 12     FLUORESCENCE ANALYSIS TEST DEVICE WITH LAMP  
MOUNTED IN INTEGRATING CAVITY (1089)
- FIGURE 13     FLUORESCENCE ANALYSIS TEST DEVICE WITH LAMP  
MOUNTED IN VACUUM BELL JAR (4019)
- FIGURE 14     CALORIMETRIC MEASUREMENT EQUIPMENT (4020)



## List of Illustrations - Continued

- FIGURE 15      SPECTRAL TRANSMISSION OF WATER (4021)
- FIGURE 16      SPECTRUM OF K-Rb LAMP WITH 50 TORR ARGON, AT  
OPTIMUM PRESSURE (4022)
- FIGURE 17      SPECTRUM OF K-Rb LAMP WITH 3000 TORR OF ARGON,  
AT OPTIMUM PRESSURE (4023)
- FIGURE 18      SPECTRUM OF K-Rb-Hg LAMP WITH 50 TORR OF ARGON  
AT OPTIMUM PRESSURE (4024)
- FIGURE 19      FLUORESCENCE POWER MEASUREMENTS FOR ALKALI  
VAPOR LAMPS AND A KRYPTON ARC LAMP (5 mm BORE,  
3 INCH ARC LENGTH) (4025)
- FIGURE 20      ARC DIAMETERS OF K-Rb ARC LAMPS 90% POINTS (4238)
- FIGURE 21      SPECTRUM OF K-Rb ARC LAMP WITH 14.5 mm BORE  
DIAMETER ENVELOPE AT HIGH PRESSURE (4486)
- FIGURE 22      SPECTRUM OF 14.5 mm K-Rb LAMP WITH NEARLY OPTIMAL  
SPECTRAL MATCHING AT 1500 W/INCH INPUT POWER (4490)
- FIGURE 23      USEFUL RADIANCE OF K-Rb and KRYPTON ARC LAMPS (4487)
- FIGURE 24      USEFUL IRRADIANCE OF K-Rb AND KRYPTON ARC LAMPS  
(4488)
- FIGURE 25      KRYPTON ARC LAMP RADIATIVE EFFICIENCY AS A FUNCTION  
OF INPUT POWER (4029)
- FIGURE 26      PERCENTAGE OF RADIATION FROM 4 mm BORE KRYPTON ARC  
LAMP ABSORBED BY 6 mm LAYER OF WATER (4030)
- FIGURE 27      DELIVERED ITEM. K-Rb LAMP IN SAPPHIRE ENVELOPE  
WITH OUTER QUARTZ JACKET, 14.5 mm BORE DIAMETER,  
8 INCH ARC LENGTH (4489)



## SUMMARY

Alkali metal vapor lamps with a bore diameter of 14.5 mm and an arc length of 8 inches, operating at 6.4 kW input power, were developed to provide a design goal of 1.6 kW of output radiation in the major pumping bands of Nd:YAG laser material. These lamps were intended as possible replacements for krypton arc lamps in a segmented-disc laser being developed elsewhere for ONR. Previous alkali metal lamps for pumping Nd:YAG with high efficiency operated with input powers up to 1 kW.

The lamps constructed in this program were limited to an outside diameter of the quartz jacket of 18 mm in order to fit the laser cavity. Constructional considerations then set the maximum bore diameter of the sapphire tube at 14.5 mm. At 8 kW the limiting parameter of the lamp is thermal wall loading.

A K-Rb mixture has been found to be the optimal alkali metal plasma material. The efficiency is optimized by adjusting the vapor pressure to provide the correct amount of broadening and self-absorption of the alkali resonance lines to match the pumping bands of the laser material.

Experimental lamps were constructed with a 14.5 mm bore diameter but only a 3 inch arc length. With constant bore diameter, input power in these lamps is known to scale linearly with arc length at constant efficiency, so the shorter lamps provided the necessary developmental data at a considerable saving over full-length lamps. Also, lamps with smaller bores and slightly different fills were constructed to determine the effects of additions to the standard K-Rb filling, and the effect of bore diameter on arc diameter and on efficiency. Krypton arc lamps were constructed for comparison with the alkali vapor lamps and for testing the measuring equipment used in the program.

The effective irradiance of the lamps was measured spectrophotometrically using a computer to calculate, in absolute units, the amount of radiation emitted by the lamp in the pumping bands of the laser material. In addition, the fluorescence excited



by the lamp in a sample of the laser material under controlled conditions was used to measure relative radiance and irradiance in the Nd:YAG pumping bands. A flow calorimeter was constructed for measuring the total radiative efficiency of the lamps.

Initially, difficulty was encountered in obtaining the correct alkali metal vapor pressure in the lamp for optimal spectral matching. The pressure was considerably too high even when the assumed cold spot was cooled to 20°C, indicating that the controlling liquid-vapor interface was at a considerably higher temperature than that of the intended cold spot. This problem was solved by enlarging the liquid metal reservoir and packing it with a wire bundle to hold the liquid metal in place by surface tension forces. With these changes, it was possible to obtain the desired vapor pressure with the external cold spot temperature only slightly lower than that corresponding to equilibrium at the observed pressure.

Lamps were operated successfully with near-optimal spectral matching up to the design level of 800 W per inch of arc length. The irradiance in the Nd:YAG pumping band was higher than that of a 10 mm bore krypton arc lamp operating at the same input power per unit length, by a factor ranging from 2 at 140 W/inch to 1.23 at 800 W/inch. The krypton arc lamp, however, had a higher radiance in the Nd:YAG pumping bands than the alkali vapor lamp by a factor of 2 at equal input powers per unit length. This fact can be correlated with the fact that the krypton lamp had an arc diameter of 4.6 mm while the alkali vapor lamp had an arc diameter of 7.4 mm. The experimental alkali lamps had an efficiency of 19% for producing radiation in the 0.7 - 0.9  $\mu$ m band. This is smaller than the contract design goal of 25% for producing radiation in this band. Since the krypton arc lamps are intended to operate at twice as high an input power as the alkali lamps, they can produce a maximum useful radiance four times as large as the alkali lamps.

Measurements on smaller bore lamps indicated that the addition of excesses of argon or mercury to the standard K-Rb filling did not increase the effective irradiance, although the spectrum of the lamp with excess mercury gave some evidence of molecular band emission on the long wavelength side of the alkali resonance lines.



An alkali vapor filled lamp was constructed with a translucent BeO envelope and was operated successfully. This was the first known alkali metal vapor lamp constructed with a BeO envelope. It eventually failed by leakage through many pinholes in the BeO envelope after operating for 16 hours. It is expected that this source of failure could be eliminated by improved manufacturing methods of the BeO envelope material.

A scaling relation was derived for optimized alkali vapor lamps. It indicates that the efficiency increases with increasing bore diameter, both at constant axial temperature and at constant input power per unit length. This result was found to hold experimentally.

At the end of the program, four prototype 14.5 mm bore, 8 inch arc length sapphire envelope, K-Rb lamps in 18 mm outside diameter quartz outer jackets were delivered.



## 1.0 INTRODUCTION AND OBJECTIVE

The objective of this program was to develop high power alkali vapor arc lamps for pumping a high power, segmented disc, axial gradient Nd:YAG laser which is being developed by another organization under ONR sponsorship.<sup>(1)</sup> The lamps to be developed had the following design goals:

Input power per lamp	6.4 kW
Output power in the 0.7 to 0.9 $\mu$ m spectral region	1.6 kW
Dimensions	
Length	8 to 10 Inches
Maximum outside diameter	1.8 cm
Operating Life	100 hours

Previous work<sup>(2)</sup> had shown that smaller-bore alkali metal vapor arc lamps were more efficient than krypton arc lamps for pumping Nd:YAG lasers at input power levels up to 1 kW, and that an efficiency of 20% or higher in producing radiation in the 0.7 to 0.9  $\mu$ m wavelength interval could reasonably be expected from this type of lamp. These 8 kW alkali vapor lamps were intended to be possible replacements for 16 kW krypton arc lamps in a laser pumping application; the higher efficiency of the alkali vapor lamps would be expected to result in a lower level of thermal dissipation in the Nd:YAG discs.

## 2.0 BACKGROUND

For the past five years arc lamps with sapphire envelopes and filled with alkali metal vapors have been investigated as efficient pumps for Nd:YAG lasers.<sup>(3,4,5,6)</sup> Sapphire lamps with quartz jackets and with protected end seals have been developed<sup>(2)</sup> and are shown in Figure 1. Laser output data show that K-Rb vapor lamps are more efficient than krypton lamps for pumping Nd:YAG, at least up to input powers of 1 kW. This is illustrated in Figure 2, which gives results for 6.2 mm bore lamps.

The limitation of 18 mm maximum outside diameter on the lamp



imposes a 14.5 mm maximum inside diameter limit on the sapphire envelope because the minimum wall thickness available in this diameter of sapphire is 0.75 mm, and a 0.5 mm vacuum gap is required between the sapphire (inner) envelope and the 0.5 mm thick quartz outer envelope. Since this lamp handles 8 kW input, the 8 inch arc length and 14.5 mm bore diameter give rise to an inner wall loading of  $88 \text{ W/cm}^2$  based on input power. It has been found previously that 100 hour lamp life can be obtained at this power level when operating in a free radiating environment.

In order to achieve the high pumping efficiency, the lamp radiation must be optimally matched to the laser excitation pump bands, as shown in Figure 3. An optimally matched K-Rb vapor lamp spectrum obtained on a prior program<sup>(2)</sup> is shown in the lower part of Figure 4.

The radiation emitted from alkali metal vapor that is useful for pumping Nd:YAG is reversed resonance radiation. Resonance radiation results from transitions between the lowest excited state and the ground state. Because the ground state is well populated, the resonance radiation emitted can easily excite another ground state atom to the first excited state. Thus the radiation and energy levels can "resonate" many times before the radiation is finally emitted from the plasma. The radiation will be increasingly trapped at higher (pressure x thickness) products as is sequentially shown in the potassium spectrum progression, Figure 5 (due to Schmidt in the pioneer study in this field<sup>(7)</sup>). The trapping results in a reversal of the center lines of the resonance radiation where the absorption coefficient is largest. The light that escapes from the plasma is in the wings of the broadened resonance lines. This phenomenon of resonance radiation reversal is used to obtain an optimal match to the Nd:YAG pump bands by adjusting the pressure in a lamp.

In arcs more than 1 inch long the emitted radiation scales linearly with power input to the arc. Thus, a 3 inch, 3 kW arc emits as efficiently as an 8 inch, 8 kW arc.

The success with which reversed radiation can be matched to the Nd:YAG bands can be demonstrated by interposing a slab of Nd:YAG material between the lamp and an emission sensor. A typical subtractive spectrum obtained by this technique, using an 0.25 inch



thick Nd:YAG slab, is shown in the upper spectrum in Figure 4. The upper trace in Figure 4 is the spectrum of the radiation emitted by this lamp that is not absorbed in a single pass through a 6 mm slab of Nd:YAG. The difference between the two curves represents the radiation absorbed by the laser material.

The wavelengths of the resonance radiation emitted by the alkali metal vapors are as follows:

Lithium	610.3 nm	670.7 nm
Sodium	589.0 nm	589.6 nm
Potassium	766.5 nm	769.9 nm
Rubidium	780.0 nm	794.8 nm
Cesium	852.1 nm	894.3 nm

Mixtures of vapors, such as a mixture of K-Rb, will display an overlap of the resonance radiation lines, and the selection of the correct alkali metal or mixture of metals will basically determine the coupling efficiency of the radiation from the arc to the Nd:YAG rod. At low vapor pressures and/or vapor thicknesses the radiation will be emitted at the resonance wavelengths, but, as discussed above, at higher pressures and/or increased vapor thicknesses it will reverse and at some point pass through the stage at which the wings of the reversed resonance radiation will match the excitation spectra of Nd:YAG. Obviously, the larger the lamp diameter the lower the pressure at which this will occur. Thus the large bore lamps used on this program should display an optimum match at a lower pressure than the 5 mm bore lamps previously investigated. <sup>(2)</sup>

As the input power per unit length of arc increases, with bore diameter held constant, the axial temperature increases. With increasing temperature, the fraction of the input power going into non-resonance lines originating from higher excited states above the resonance level increases. Since these non-resonance lines do not in general contribute to pumping the laser material, it is desirable to keep the plasma temperature as low as possible. Larger bore lamps are advantageous from this standpoint since, for a given input power per unit length, the axial temperature decreases with



increasing bore diameter.

From this brief review we can see that the lamp parameters pertinent to this work are:

1. the plasma material
2. the alkali metal vapor pressure
3. within certain limits, the bore diameter
4. within certain limits, the length of the lamp
5. the input power per unit length
6. also, active or inactive additions to the alkali metal vapor, such as mercury and argon, which may affect the performance of the lamp.

### 3.0 EXPERIMENTAL APPROACH

Development of an efficient 8 kW lamp represents a significant advance in alkali metal laser pump technology, as the most advanced lamp previously developed has an 8 mm outside diameter, a 3 inch arc length, and a 1 kW power limitation.

At the start of this program it was not known whether the effects on spectral output of increasing the bore diameter could be compensated for by adjusting the other allowable lamp parameters to maintain the necessary line reversal. Therefore, alternatives were considered for reducing bore diameter by increasing the wall loading capability of the lamp. These were the use of thinner wall sapphire lamps, and the use of beryllium oxide envelopes. In both cases the thermal stress resistance of the lamps could be increased. Sapphire tubing in the required bore diameter with walls thinner than 0.76 mm were not available at the start of this work, but beryllium oxide in translucent polycrystalline form could be obtained and one small bore lamp was constructed of this material for evaluation.

In addition, 5 mm and 6.3 mm bore, 3 inch arc lamps (identical with those used on a prior alkali metal program<sup>(2)</sup>) were used (a) to determine whether the addition of mercury or argon would increase the



laser pumping efficiency of K-Rb lamps; and (b) to compare their arc sizes with those of larger lamps, as part of power density and radiance studies. Since both input power and radiative output scale linearly with arc length for lengths greater than about 1 inch, lamps with 14.5 mm bore and 3 inch arc length were used during the initial development in order to lower lamp fabrication costs and allow the use of lower-power test equipment. (The final delivered lamps had an arc length of 8 inches.)

Krypton arc lamps of several designs and bore diameters were also constructed for comparison with the alkali vapor lamps.

#### 4.0 EXPERIMENTAL PROCEDURE

##### 4.1 Lamp Construction

##### 4.1.1 Alkali Metal Vapor Lamps

All but one\* of the alkali vapor lamps were made of drawn sapphire envelopes (from Tyco) and niobium + 1% zirconium end caps, tantalum tubulations, and tungsten electrodes. The construction followed the fabrication processes previously developed.<sup>(2)</sup> The 5 mm and 6.3 mm bore by 3 inch arc length lamp structures are shown in Figure 1. The cross-section diagram of the 14.5 mm bore, 3 inch arc length lamp with the final reservoir configuration is shown in Figure 6, together with a drawing of this type of lamp enclosed in a quartz envelope. The 8 inch arc length lamps delivered at the end of the program also followed the design shown in Figure 6. The end caps are sealed to the sapphire using an active alloy at 1350°C. The alkali metal is introduced into the lamp via one of the tantalum tubulations, which is then pinched off and electron-beam welded. During operation, the end of one of the tubulations becomes the cold spot of the lamp and the reservoir for the unvaporized alkali metal. The cold spot normally controls the vapor pressure of the alkali metal within the

---

\*One lamp was made with a BeO envelope.



lamp. In the 5 mm and 6.3 mm bore lamps the vapor pressure is controlled by heating or cooling the cold spot tubulation. In the large lamps the vapor pressure is controlled by a forced-convection water-cooled arrangement that cools a copper block which, in turn, is in intimate contact with the cold spot of the lamp, as shown in Figure 7. For lamps protected by quartz jackets, split carbon blocks provide the thermal path from the lamp cold spot to the outside world. The quartz outer envelope is shrunk down over the carbon to provide a continuous conduction path. The shrunk-down quartz region can be heated with a spiral nichrome heater or cooled by forced air convection.

The lamps are started with a high voltage low current pulse of 20,000 volts. A low pressure (50 Torr) argon fill assists in arc initiation. The lamps are then gradually brought up to power over a several-minute period in order to allow the alkali metal to vaporize and to form a stable arc, and to minimize transient thermal stresses on the sapphire envelope. A dc power supply is normally used for this operation. An alkali metal lamp requires "seasoning" for the first hour of its operation, after which the measurements described in the next section may be performed.

Small bore alkali metal lamps were constructed with the standard fill found to be optimum on a prior program,<sup>(2)</sup> i.e., a 50:50 mix of K-Rb with a 50 Torr addition of argon starter gas. Two lamps were also constructed with a variation of this fill. 3000 Torr of argon was added to the K-Rb fill in one lamp, and mercury was added to the K-Rb fill in the other lamp.

One lamp was also constructed with a translucent polycrystalline beryllium oxide envelope. It had a 5 mm bore diameter, a 3 inch arc length and was filled with the standard K-Rb-argon mixture. The potential usefulness of beryllium oxide as an envelope material for high power alkali vapor lamps



is based upon its high thermal conductivity, high melting point, and superior resistance to chemical attack by hot alkali metals. The thermal conductivity allows a BeO envelope to operate at higher wall loadings and greater rates of temperature change (i.e., shorter startup and shutdown cycle times) than an alumina envelope, without cracking because of thermal stresses. In addition, the greater chemical stability of BeO should result in an increased life, as compared with alumina, when both materials are operated at the same temperature.

At the beginning of this program translucent BeO was not available in the form of tubes suitable for lamp envelopes so the envelope was fabricated from a solid slab of the material by core drilling and polishing, and the metallizing technique for the brazing operation was developed using the residual pieces. The lamp was successfully fabricated and was operated for 16 hours at 500 W input power. This was the first reported instance of the successful construction and operation of an alkali metal lamp with a beryllium oxide envelope.

#### 4.1.2 Krypton Lamps

Standard ILC externally-water-cooled lamps of 4, 6, and 10 mm bore diameter and 3 inch arc length were constructed and filled to 3 atmospheres. A new type of krypton lamp with electrodes internally cooled by water, but still capable of being processed at high temperatures, was constructed with 10 mm bore diameter. This lamp was designed to maintain lower electrode temperatures than the standard (externally water cooled) lamps. It was tested initially at 3 atmospheres fill, and later filled to 7 atmospheres. These krypton lamps are illustrated in Figures 8, 9, and 10.

The krypton lamp with internally water-cooled



electrodes was life tested and was found to have an operating lifetime of 500 hours, which is 6 to 12 times greater than the lifetime of externally cooled krypton arc lamps.

#### 4.2 Spectral Measurements

##### 4.2.1 Absolute Spectral Irradiance Measurements

The absolute spectral irradiance measurements on the alkali vapor and krypton lamps were made with the procedures recommended by the N.B.S. (8) The spectral irradiance measurements together with the calorimetric measurements, specify the electro-optical conversion efficiency of the lamps in the 0.7 to 0.9  $\mu\text{m}$  wavelength interval band. An alkali vapor lamp is mounted in a Pyrex vacuum bell jar for making spectral irradiance measurements. The mounting is keyed to an optical bench so that the lamp is precisely and reproducibly aligned to the detector system, which is mounted at 50 cm distance from the lamp.

Emission spectra were taken at 10 $\text{\AA}$  intervals with a Jarrell Ash 1/4 meter monochromator, using a photomultiplier detector with an extended-range S-1 phosphor. The system response was initially determined using an Eppley standard irradiance lamp (traceable to NBS) as a reference, mounted in the pyrex vacuum bell jar used for alkali vapor lamps.

All output data were digitized and punched onto paper tape for input to a computer program. The system transfer functions are also stored in the computer program. Execution of the program resulted in corrected data plotted on an XY recorder, over the range of 0.4  $\mu\text{m}$  to 1.6  $\mu\text{m}$ . Time-shared computer processing allows a rapid (approximately 3 minute time lag) determination of the spectral irradiance in this 0.4  $\mu\text{m}$  to 1.6  $\mu\text{m}$  band.



#### 4.2.2 Relative "Effective" Irradiance Measurements

In addition to the measurement of spectral irradiance several relative measurement techniques were developed for use with lamps for pumping lasers. The first technique involves a computerized integration of the spectral irradiance curve multiplied by the absorption coefficient, at each wavelength, of Nd:YAG, which has been previously digitized and entered into the computer program. The quantity that is obtained is the effective spectral irradiance of the lamp, and is measured in terms of watts per  $\text{cm}^2$  per nanometer per unit thickness of laser material for a single pass of lamp radiation. A block diagram of the equipment used in this operation is shown in Figure 11.

A second special technique involves measurement of the effective irradiance emitted from a lamp by using a differential Nd:YAG fluorescence analysis method. This method was first devised for use in a cylindrical integrating cavity arrangement for low power lamp measurements, and has previously been described in detail.<sup>(2)</sup> A schematic diagram of this arrangement is in Figure 12. The integrating cavity technique was used to take measurements on the small bore lamps evaluated on this program.

The fluorescence analysis technique was adapted to enable measurements to be carried out to the 8 kW level. This modified arrangement is shown in Figure 13. The integrating cavity arrangement is replaced with a direct irradiance measurement of the lamp as it is operated in the vacuum bell jar. A precision holder was fabricated so that the two radiation sensing units could be positioned at a precise distance from the lamp. The sensors are mounted external to the bell jar. They consist of 0.25 inch thick undoped YAG and doped Nd:YAG rectangular slabs of material, behind each of which is placed



a 1.06  $\mu$ m transmission filter and a PIN diode. The PIN diodes convert any radiation impinging on them to a millivoltage. The scattered light signal from the diode behind the undoped YAG is electrically subtracted from the fluorescence plus scattered light signal produced by the other diode. A relative measure of the amount of lamp radiation that is converted to 1.06  $\mu$ m fluorescence radiation is thus obtained in terms of a fluorescent output voltage (FOV).

The use of this FOV technique provides a rapid iterative technique for optimizing a lamp at a given power level by progressively adjusting the cold spot temperature, and thus the pressure and voltage gradient in the lamp, and plotting the FOV reading against input power at constant current. The FOV maximum on this curve corresponds to an optimum match of the alkali metal lamp to the Nd:YAG material. This procedure can be carried out from the ignition point of the lamp up to the highest operating point at which the lamp can be safely operated. A curve is obtained somewhat similar to a laser slope efficiency curve. Plots of FOV versus lamp input power can be compared for different lamps, and their relative effective irradiances can be determined.

This device has previously proven itself as a means of providing a rapid lamp selection technique to the point where now, at ILC, it is used before other photometric tests are performed. Spectra are then taken at the lamp operating conditions corresponding to the maximum FOV reading, and occasionally also at operating points on each side of this condition in order to confirm the FOV data by examining the under-reversed and over-reversed operating conditions.



#### 4.2.3 Relative "Effective" Radiance Measurements

Useful radiance measurements were made in the same manner. An image of the arc was formed by means of a quartz lens and a slit mounted in front of the sensing Nd:YAG crystal. The resulting FOV signal is a relative measure of the amount of useful radiation per  $\text{cm}^2$  of projected area and per steradian, emitted by the arc along a ray intersecting the arc axis and at a right angle to the axis. The concept of radiance is not strictly applicable to the arcs studied in the present work, since these arcs are not optically thick over most of the wavelength range of the emitted light. However, an effective radiance can be defined in the manner just indicated.

#### 4.3 Calorimetric Measurements

Calorimetric measurements were made to determine the total, and the 0.3 to 1.3  $\mu\text{m}$ , radiative efficiency of the krypton and the alkali vapor arc lamps. In conjunction with a relative irradiance measurement over the 0.3 to 1.3  $\mu\text{m}$  region, these measurements can then be used to obtain the lamp radiation efficiency in any band within this range, such as the 0.7 to 0.95  $\mu\text{m}$  band.

A diagram of the experimental arrangement for making calorimetric measurements on a water cooled krypton lamp is shown in Figure 14. The lamp is centered in a quartz water jacket of 1 mm wall thickness, with a gap of about 1 mm between the outside of the lamp and the inside of the water jacket. Cooling water flows through the gap at a rate of 1.0 gal/min. The cooling water temperature is 15° to 20° C. The flow rate is monitored by flowmeter 1 and the increase in temperature of the cooling water is given by the difference in the readings of thermometers 1 and 2. This allows calculation of the envelope and electrode heat dissipation,  $P_h$ . The radiative output is measured by absorption in a calorimeter constructed from two concentric lengths of quartz tubing



with a 6 mm annular spacing. Water, either clear or made opaque by the addition of India ink, is circulated through the calorimeter, flowmeter 2, and a heat exchanger. The rise in temperature due to absorption of radiation by the 6 mm layer of water is given by the difference in the readings of thermometers 3 and 4. The flow rate, which is maintained at about 0.6 gallons per minute, is monitored by flowmeter 2. This allows calculation, with the use of opaque water, of the total radiated power,  $P_r$ , and with clear water the amount of power outside the  $0.3 - 1.3 \mu\text{m}$  region. According to the curve of water absorption plotted against wavelength, which is shown in Figure 15,<sup>(9)</sup> the radiation outside of the  $0.3 - 1.3 \mu\text{m}$  region will essentially all be absorbed by a 6 mm thick water layer. The input power to the lamp is calculated from lamp voltage and current measurements ( $V \times I$ ). The efficiency is given by  $P_r / (P_r + P_h)$ , and a check on the accuracy of the measurements is possible through the fact that the  $V \times I$  product should be equal to  $P_r + P_h$ . For each lamp, a series of readings is taken at different input power levels.

#### 4.4 Arc Diameter Measurements

The arc image was projected directly onto a screen and the diameter of the plasma was measured as a fraction of the cross section of the sapphire envelope. Then, knowing the diameter of the envelope, the arc diameter is determined. The alkali metal lamps used for this test, as for the calorimetric test, were enclosed in quartz jackets as shown in Figure 1 and Figure 6.

### 5.0 EXPERIMENTAL RESULTS\*

#### 5.1 Results For 5 mm and 6.3 mm Bore, 3 Inch Arc Length Alkali Metal Vapor Lamps

The small bore alkali metal lamps were operated in evacuated quartz envelopes. Cooling of the inner sapphire

---

\*The lamp numbers cited in this section refer to a recorded, chronological, sequential numbering of all developmental alkali metal lamps constructed at ILC.



envelope was by radiation; cooling of the outer quartz envelope was by free air convection. The cold spot temperature was regulated as discussed in the previous section. Details of the operation of lamps of these sizes have been discussed previously.<sup>(2)</sup> Their construction details are shown in Figure 1.

The beryllium oxide envelope lamp, as described in Section 4.1.1, was operated successfully for 16 hours at 500 W input power. It failed after 16 hours by multiple pinhole leaks appearing in the center (highest temperature) portion of the envelope. This mode of failure has often been noted in polycrystalline alumina envelope lamps<sup>(2)</sup> and apparently can be overcome by improved ceramic manufacturing techniques. About this time work under another contract was started to evaluate large diameter BeO lamps for pulsed applications<sup>(10)</sup>, so work on BeO lamps in the present program was not carried further.

It should be noted that, since the BeO envelopes are translucent, the effective radiating surface is the exterior of the envelope. Thus the radiance (brightness) of the lamp for laser pumping will be lower than when transparent sapphire envelopes of the same O.D. are used. However, because of the greater thermal shock resistance, smaller lamps can be fabricated and operated.

Transparent sapphire envelope lamps were constructed with 5 mm bore and 3 inch arc lengths. These lamps were filled with K-Rb + 50 Torr of argon (No. 138), K-Rb + 3000 Torr of argon (No. 78), and K-Rb (5 mg) + Hg (50 mg) + 50 Torr argon (No. 131). Spectral data for these lamps is presented in Figures 16, 17, and 18. The integrated area of the spectrum that matches the pump bands of Nd:YAG was measured, and the areas were found to be equivalent for all three lamps.

FOV data were taken on the K-Rb and the K-Rb + Hg lamps. These comparative data are shown in Figure 19 and the FOV results are shown to be similar. FOV data was not taken on the 3000 Torr argon lamp, No. 138 as the primary



point being explored with this lamp was the shift of the reversed resonance lines of the alkali metal species. No shift was noted.

Lamp No. 131, with Hg in addition to the standard K-Rb fill material, was operated with square-wave alternating current at 0.5 to 20 kHz in order to prevent separation of the fill components by electrophoresis. The data in Figure 19 show that the lamp with mercury added is superior to a lamp with the standard filling when both are operated on square-wave alternating current. However, the K-Rb lamp operated dc has slightly higher pumping efficiency than the ac-operated K-Rb-Hg lamp and, in addition, does not require a special square-wave ac power supply. Therefore the development of the mercury additive lamps was not pursued further.

The calorimetric equipment described in Section 4.3 was used to measure the total radiative efficiency of a quartz-jacketed 5 mm bore, 1.9 inch arc length, K-Rb lamp. It was found that 87% of the input electrical power was radiated, the remaining 13% being lost by conduction through the electrical leads and by conduction and convection from the quartz jacket to the surrounding air. A measurement with water only (no black dye) in the calorimeter gave the result that 51% of the input power was absorbed by the water under these conditions. This represents radiated power at wavelengths smaller than  $0.3 \mu\text{m}$  and greater than  $1.3 \mu\text{m}$ . Spectral irradiance measurements on the same lamp, carried out as described in Section 4.2.1, indicated that 25% of the input power was radiated between  $0.7$  and  $0.9 \mu\text{m}$ , the wavelength range that includes the major pumping bands of Nd:YAG, and that an additional 11% of the input power was radiated in infrared lines between  $0.9$  and  $1.3 \mu\text{m}$ . The power distribution in this lamp, operating at 54 W per cm of arc length, is therefore as shown in Table I.



TABLE I

## POWER DISTRIBUTION IN LAMP

<u>Dissipation Mechanism</u>	<u>Percent of Input Power</u>
Conduction through leads (estimated)	5%
Conduction and convection from envelope (estimated)	8%
Radiated:	
0.7-0.9 $\mu\text{m}$ (from spectral irradiance)	25%
0.9-1.3 $\mu\text{m}$ (from spectral irradiance)	11%
0-0.3 and 1.3-10 $\mu\text{m}$ (from water absorption)	51%
Total	100%

The results of the measurements of the arc diameters of the alkali metal plasmas, plotted against input power to the lamp, are presented in Figure 19.

#### 5.2 Results for 14.5 mm Bore, 3 Inch Arc Length, K-Rb 50 Torr Argon Filled Alkali Metal Vapor Lamps

Lamps with an arc length of 3 inches and a bore diameter of 14.5 mm were constructed of Tyco drawn sapphire tubing according to the general design shown in Figure 6. In the first lamp constructed, communication between the tubulation and the interior of the lamp was by means of a hole drilled through the side of the electrode body near the sapphire wall. During initial startup a locally high concentration of alkali metal liquid and vapor was present at the exit of this hole and on the surface of the sapphire, resulting in formation of an arc which terminated on the sapphire wall. The resulting local heating of the sapphire wall near the seal caused a crack to develop at this point, and the lamp failed.



The second lamp had the pumping and filling hole drilled axially through the electrode instead of through the side. This lamp was operated successfully up to 1 kW input power, but the spectrum shown in Figure 21 indicated that the lamp was being operating at considerably too high a pressure of alkali metal vapor to produce optimal matching of the reversed resonance lines to the Nd:YAG absorption bands, even when the external surface of the tubulation was cooled to 0°C. It was suspected that the pressure of alkali vapor inside the lamp was unable to reach equilibrium with the liquid at the cold-spot temperature because the communicating hole through the electrode had inadequate conductance for vapor flow. It was further theorized that liquid alkali metal was being transported by surface tension forces along the inside surface of the reservoir to regions of considerably higher temperature than the intended cold spot temperature, thus effectively increasing the cold spot temperature.

Accordingly, subsequent lamps were modified by increasing the diameter of the reservoir to 0.2 inches. The reservoir was tightly packed with a bundle of 0.010 inch diameter titanium wires in the cooler end. The diameter of the reservoir was increased to provide adequate vapor conductance, and the wire bundle was intended to act as a wick and retain the liquid metal.

The lamp with this modified reservoir was mounted into a copper block for thermal control. The copper block could be heated electrically or cooled by forced air convection as required to maintain the desired cold spot temperature. The lamp was ordinarily operated with this reservoir electrode serving as the cathode. The other end of the lamp was cooled by radiation, and was intended to reach a higher temperature than the reservoir.

Lamps of the modified design were operated successfully at input levels up to the design goal of 2.4 kW for a 3 inch arc length, corresponding to 6.4 kW for an 8 inch arc length. Satisfactory control of the cold spot temperature was obtained



with forced air cooling of the copper mounting block. The spectrum of a lamp operating at an input power of 1.5 kW is shown in Figure 22. Comparison with Figure 4 indicates that the pressure was slightly too high, i.e., the lines were slightly over-reversed, at the time the spectrum in Figure 22 was taken. The cold spot temperature, measured with a thermocouple in contact with the outer surface of the electrode stem at the level of the end of the wire bundle, was 518°C. At this temperature the vapor pressures of potassium and rubidium are 40 Torr and 100 Torr, respectively. The displacement of the peak of the reversal wing in Figure 22 from the center of the potassium resonance line on the short wavelength side is 15 nm. This displacement can be correlated with the pressure of alkali metal by a method described by Jen, Hoyaux, and Frost,<sup>(11)</sup> and corresponds to an alkali metal vapor pressure of about 100 Torr. This implies that the pressure of alkali metal vapor in the lamp was in equilibrium with liquid alkali metal at a temperature only slightly greater than the measured cold spot temperature.

The spectral irradiance of a 14.5 mm bore diameter, 3 inch arc length K-Rb lamp was measured at an input power of 870 W, or 114 W per cm of arc length. Determination of the area under the spectral irradiance curve over the wavelength interval 0.7-0.9  $\mu\text{m}$  indicated that a 19% of the input power was radiated in this wavelength interval, which includes the principal pump bands of Nd:YAG. An additional 11.5% of the input power was radiated in the wavelength region between 0.9 and 1.4  $\mu\text{m}$ . Thus, the 14.5 mm bore lamp is less efficient in producing radiation in the 0.7-0.9  $\mu\text{m}$  interval than the 5 mm bore lamp, which radiated 25% of the input power in this interval, as reported in Section 5.1.

The theoretical scaling relation presented in Section 6.1, below, suggests that, at constant input power per unit length, both the total radiative efficiency and the efficiency for producing resonance radiation should increase with increasing bore diameter. Consequently it should be noted here that the comparison just made was between a 14.5 mm lamp operating at 114 W/cm and a 5 mm lamp operating at



54 W/cm. The larger value of power per unit length in the 14.5 mm lamp results in a higher plasma temperature, and this causes a larger fraction of the radiated power to be emitted in non-resonance lines outside of the 0.7-0.9  $\mu\text{m}$  region.

A comparison of useful radiance (for pumping Nd:YAG) was made between a 14.5 mm bore K-Rb lamp and a 10 mm bore krypton arc lamp (the size used in the Nd:YAG slab laser), using the FOV technique described in Section 4.2.3.

The comparison of useful effective radiance between the two lamps is shown in Figure 23. Since both lamps had the same arc length, the comparison is made by plotting the FOV reading against input power instead of against input power per unit length, which would be the appropriate independent variable if lamps with different arc lengths were being compared. It is apparent that the useful effective radiance of the krypton arc is nearly twice as large as that of the alkali metal arc at input powers near 2 kW. This difference can be correlated with the fact that the arc diameter, measured visually as described in Section 4.4, was 4.6 mm for the krypton arc and 7.4 mm for the K-Rb arc.

The useful irradiance, (i.e., the amount of useful light falling on a receiver at a specified distance from the source, per unit area of receiver surface normal to the direction of the light), of the two lamps was also compared by means of the FOV technique described in Section 4.2.2. The results of the comparison are given in Figure 24. Here the total input power is the appropriate independent variable even if the lamps being compared have different arc lengths or diameters. The alkali vapor lamp has a larger useful irradiance than the krypton lamp, by a factor ranging from 2 at 140 W/inch to 1.23 at 800 W/inch. In making the radiance and irradiance comparisons, both the alkali lamp and the krypton lamp were operated inside a Pyrex bell jar, so that the optical path between the lamp and the measuring device was the same for both lamps.



### 5.3 Results for 4, 6, and 10 mm Bore, 3 Inch Arc Length, 3 Atmosphere Filled Krypton Arc Lamps

The useful radiance and irradiance of the 10 mm bore krypton arc lamp (for pumping Nd:YAG) were compared with the useful radiance and irradiance of the 14.5 mm bore K-Rb lamp as described in Section 5.2, and the results of the comparison are shown in Figures 23 and 24.

Krypton arc lamps with electrodes externally cooled by water were used to test the water calorimeter equipment constructed during this program. Krypton arc lamps were used because another efficiency measuring system, not compatible with alkali metal lamp operation, was available for checking the results. The cross check of the results gave an agreement of the total radiative efficiency to within 1%.

The total radiative efficiency of the krypton lamps as a function of input power, up to a maximum of 4 kW, is given in Figure 25. The results of the calorimetric tests confirm the data reported in the literature,<sup>(12)</sup> i.e., the radiative efficiency increases with both lamp bore diameter and lamp input power. The percentage of radiation from the 4 mm bore lamp that is absorbed in the 6 mm water thickness of the calorimeter is plotted against lamp output power in Figure 26. At the 4 kW lamp input power level, 46% of the input power is radiated; 7% of the input power is absorbed in the 6 mm water layer of the calorimeter.

The power balance of the lamp is therefore as follows:

Heating of envelope and electrodes	54%
Radiated 0.3 to 1.3 $\mu\text{m}$	39%
Radiated at wavelengths beyond 1.3 $\mu\text{m}$	7%
	<hr/>
Total Input Power	100%
	<hr/>



## 6.0 DISCUSSION

### 6.1 Performance of Large-Bore Alkali Vapor Arc Lamps in Pumping Nd:YAG Laser Material

Potassium-rubidium arc lamps with sapphire envelopes of 14.5 mm bore diameter and arc lengths of up to 8 inches were successfully constructed and operated at input power levels up to 800 W per inch of arc length, with optimal spectral matching to the pump bands of Nd:YAG. (As far as is known, these are the largest alkali vapor arc lamps ever constructed.) Thus, the contract design goals for the size and input power capability of the lamps were achieved. However, the contract design goal of 25% efficiency in producing radiation in the  $0.7 - 0.9 \mu\text{m}$  wavelength interval was not realized; the measured efficiency in producing radiation in the  $0.7 - 0.9 \mu\text{m}$  interval was only 19%.

These lamps had a larger useful irradiance for pumping Nd:YAG than the 10 mm bore krypton arc lamps which they were intended to replace, when both lamps were operated at the same input power. However, the useful radiance of the alkali lamps was smaller than that of the krypton arc lamps when both lamps were operated at the same input power per unit length, because the diameter of the arc was larger in the alkali arc than in the krypton arc. Because of this fact, the use of large alkali vapor lamps in the originally intended laser pumping application is not presently being pursued. However, four full-size 8 inch arc length lamps were constructed and delivered for testing in a laser cavity at some future date.

### 6.2 Scaling Relations for Resonance Radiation-Dominated Arcs

The data plotted in Figure 24 show that a 14.5 mm diameter K-Rb lamp produces a considerably higher useful irradiance (for pumping Nd:YAG) than a 5 mm bore lamp at the same input power. In order to understand this result and determine whether it can be explained theoretically, an efficiency



scaling relation for alkali vapor arcs was derived and is presented in this section. The scaling relation indicates that, at constant input power per unit arc length, the efficiency increases with bore diameter, in agreement with the experimental observation.

Let  $R$  be the radius of the plasma boundary (the inside surface of the lamp envelope) and let  $r$  be the radius at any point in the interior of the plasma. Then the temperature distribution,

$$T = T(r) \quad (1)$$

can be expressed in the form

$$T(r) = T(r/R) \quad (2)$$

It is shown in Appendix A that the radiative energy flux,  $F_r$  in  $\text{W}/\text{cm}^2$  at the plasma boundary is proportional to  $R^{1/2}$  if  $R$  is changed while keeping the temperature distribution,  $T(r/R)$  unchanged

$$F_r = a_1 R^{1/2} \quad (3)$$

where  $a_1$  is a constant.

This result is true for both resonance and non-resonance lines as long as the lines are isolated, so that radiation in the wings of one line is not significantly absorbed by neighboring lines. (Close multiplets such as the alkali resonance doublets can be treated as single lines with suitable averaging of the transition probabilities.)

The energy flux due to heat conduction at the plasma boundary,  $F_c$  is equal to

$$F_c = K \frac{dT}{dr} = \frac{K}{R} \frac{dT}{d(r/R)} \quad (4)$$



where  $K$  is the heat conductivity. Thus,  $F_c$  is proportional to  $1/R$  if  $R$  is changed while keeping the temperature distribution unchanged:

$$F_c = a_2/R \quad (5)$$

where  $a_2$  is a constant.

Under these circumstances, the ratio of radiated to conducted energy flux, which is equal to  $\eta/(1-\eta)$ , where  $\eta$  is the radiative efficiency, is given by

$$\frac{\eta}{1-\eta} = \frac{a_1}{a_2} R^{3/2} \quad (6)$$

It has been shown (11) that the displacement from the line center of the intensity maxima of the wings of the reversed resonance lines is proportional to  $pR^{1/2}$ , where  $p$  is the pressure. This displacement must remain constant if the bore diameter of the lamp is changed and the pressure is readjusted to maintain the optimal match of the lamp spectrum to the absorption bands of the laser material. Thus, for optimized lamps,  $p$  is proportional to  $R^{-1/2}$  and  $\frac{\eta}{1-\eta}$  is proportional to  $R$ .

The constant  $a_1$  in Equation (3) is approximately proportional to  $pT_0^{3/2}$  for resonance lines, where  $T_0$  is the temperature at the axis of the arc, as is seen from Equation (23) of Appendix A. In this equation the quantity  $k_0(0)w(0)$  is proportional to  $p^2/T_0^2$ , and the quantity  $B(0)$  is proportional to  $T_0$  at high temperatures.

For non-resonance lines the constant  $a_1$  is approximately proportional to  $p$  and to an exponential function of  $T_0$ . Therefore optimized lamps obey the relation

$$F_r = a_3 (T_0^{3/2} + f(T_0)) \quad (7)$$

where  $a_3$  is a constant.



The heat conduction flux at the wall is independent of pressure and is proportional to  $T_0/R$ . For optimized lamps the total power,  $P$ , obtained by adding the radiative and heat conduction fluxes and multiplying by the surface area of the plasma, which is proportional to  $RL$ , where  $L$  is the arc length, is therefore of the form

$$P = \{a_4 (T_0)^{3/2} + f(T_0) R + a_5 T_0\} L \quad (8)$$

where  $a_4$  and  $a_5$  are constants.

Equation (8) is the scaling relation for optimized alkali vapor lamps. It indicates that, at constant axial temperature and arc length, the radiated power is proportional to  $R$  while the conducted power is independent of  $R$ . Therefore, under these circumstances, the radiative efficiency and the total power both increase as  $R$  increases.

If, instead, the total power and the arc length are held constant while increasing  $R$ , the axial temperature decreases. The radiative efficiency is equal to

$$\eta = \frac{P/L - a_5 T_0}{P/L} = 1 - \frac{a_5 T_0 L}{P} \quad (9)$$

This indicates that at constant  $P/L$  also, the radiative efficiency increases with increasing  $R$ , because of the decrease in  $T_0$  resulting from increasing  $R$ . The efficiency for producing resonance radiation increases even more, because the term in Equation (8) corresponding to non-resonance radiation decreases more rapidly than the resonance radiation term with decreasing temperature.

The predictions of this analysis are borne out by the data plotted in Figure 24. Similar results have been obtained by Lowke<sup>(13)</sup> from numerical solutions of the equations of radiative transfer and power balance in sodium vapor lamps.



### 6.3 Control of Vapor Pressure

In the early part of this program difficulty was encountered in obtaining the correct pressure of alkali metal vapor for optimal spectral matching in the 14.5 mm bore lamps. The pressure was considerably too high even when the external surface of the intended cold spot was maintained at 40°C. It was hypothesized that liquid metal was being transported along the inside surface of the tubulation by surface tension forces, so that equilibrium between liquid and vapor was reached at a point where the temperature was much greater than the intended cold spot temperature. In other words, the tubulation was acting as a heat pipe. Design modifications suggested by this hypothesis, i.e., enlarging the diameter of the reservoir and packing its end with a wire bundle to retain the liquid metal in place, proved successful in making it possible to obtain the pressure required for spectral matching, with the external cold spot temperature only slightly lower than the temperature corresponding to liquid-vapor equilibrium at the observed pressure (as calculated from the degree of broadening of the resonance lines).

A review of data obtained earlier on smaller lamps<sup>(2)</sup> indicated that the same problem had occurred there also. Measured external cold spot temperatures were several hundred degrees lower than those corresponding to equilibrium at the pressure inferred from line broadening. In these smaller-bore lamps this did not represent a serious problem, however, because a higher pressure was required for optimal spectral matching.

### 6.4 Effect of Increased Argon Pressure

Increasing the argon pressure from 50 Torr to 3000 Torr did not affect the position of the reversed radiation wings of the optimally matched K-Rb, 6.3 mm bore lamps. If the radiation had been due to excited K<sub>2</sub>, Rb<sub>2</sub>, or K-Rb molecules, a shift of the radiative peaks would have occurred due to a higher concentration of excited molecular vibrational



states. We conclude that the resonance radiation is due to excited atoms. (In contradistinction the radiation emitted from high pressure, 1000 Torr pulsed lamps is due to a mixture of excited atoms and molecules.)

#### 6.5 Effect of Adding Mercury

The addition of mercury to a K-Rb lamp does not increase the effective irradiance. It does raise the general level of background radiation and also seems to broaden out the long wavelength wing of the reversed resonance radiation. (This latter phenomenon had been noted previously.<sup>(3)</sup>) This broadening may be due to the appearance of KHg and RbHg molecules, as the pressure of Hg at 500°C is several atmospheres. In addition, the arc diameter appears to be smaller in the lamp with added mercury.

#### 6.6 Beryllium Oxide Envelope Lamps

The use of BeO as an envelope material offers the long range possibility of reducing the bore size of the present 14.5 mm bore K-Rb sapphire envelope lamp by increasing the maximum permissible thermal wall loading. A reduced bore size means a physically thinner alkali metal vapor layer through which the resonance radiation must pass, thus enabling an irradiance match to the laser rod to be made at a higher lamp vapor pressure. A thinner walled sapphire envelope would serve a similar purpose as it, too, could handle high thermal wall loadings.

#### 6.7 Radiative Efficiency of Krypton Arc Lamps

At high power levels, the total radiative efficiency of krypton lamps approaches 50%, and the radiation in the 0.3 - 1.3  $\mu\text{m}$  band is of the order of 39% of the input power. The power density of the lamps can be computed from arc diameter measurements. This information can provide basic information to further understanding of krypton arc radiative processes.



7.0 CONCLUSIONS

The following major conclusions can be drawn from the work performance under this contract:

1. Potassium-rubidium arc lamps with sapphire envelopes of 14.5 mm bore diameter were constructed and successfully operated at input power levels up to 800 W/inch of arc length, the original contract design goal, with optimal spectral matching to the pump bands of Nd:YAG.
2. The efficiency of these lamps for producing radiation in the 0.7 - 0.9  $\mu$ m wavelength interval was 19%. This is smaller than the contract design goal of 25% efficiency for producing 0.7 - 0.9  $\mu$ m radiation.
3. These lamps had a larger useful irradiance for pumping Nd:YAG than the 10 mm bore krypton arc lamps which the 14.5 mm alkali vapor lamps were intended to replace, when both lamps were operated at the same input power per unit length.
4. The useful radiance of the 14.5 mm K-Rb lamps for pumping Nd:YAG was smaller than that of the 10 mm krypton lamps when operated at the same input power per unit length, because the krypton arc had a smaller diameter than the alkali vapor arc.
5. The addition of excesses of argon or mercury to the standard K-Rb fill does not improve the spectral matching or the efficiency of pumping Nd:YAG laser material.
6. BeO was successfully tested as an alternative to sapphire for use as an envelope material in constructing alkali vapor arc lamps. Because of its higher thermal stress resistance the use of BeO should permit a reduction in bore diameter at a given input power per unit length.



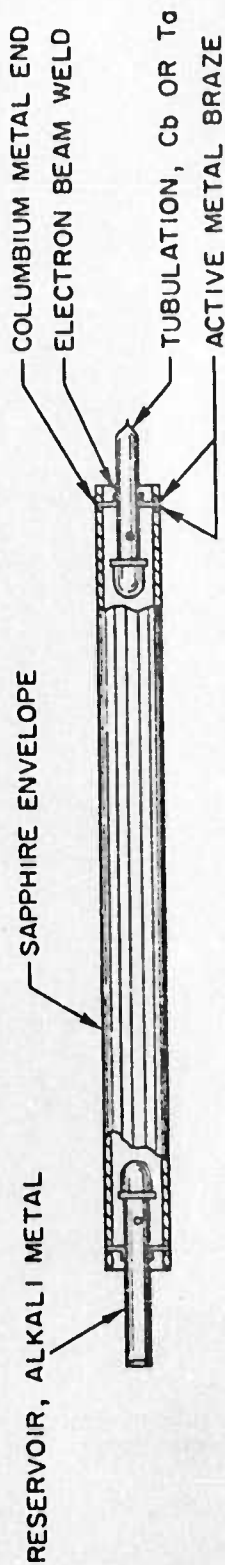
LITERATURE CITED

1. I. H. Taylor, I. Liverman, R. Liebermann, A. Federowicz, I. Armstrong, Jr., "Optical Pumping of Lasers, Final Report Technical Report No. 3, June 1969 to March 1970", ARPA Contract No. N00014-69-C-0428, May 1970, p. 31, Korad, Division of Union Carbide, NRL Contract No. XN00014-70-C-0406.
2. I. Noble, J. Moffat, I. Reed and J. Richter, "Optical Pumps for Lasers", Final Report, May 1971, Contract No. DAAB07-70-C-0035.
3. I. Liberman, D. A. Larson, C. H. Church, "Efficient Nd:YAG Lasers Using Alkali Additive Lamps", IEEE J. Quant. Elect. QE-5, 238 (1969).
4. I. Liberman, et al., "Optical Pumps for Lasers - Phase II, Final Report", Contract DA-28-043-AMC-02097 (E) 1968.
5. I. H. Taylor, I. Liberman, R. Liebermann, A. Federowicz, I. Armstrong, Jr., "Optical Pumping of Lasers, Final Report, Technical Report No. 3, June 1969 to March 1970", ARPA Contract No. N00014-69-C-0428, May 1970, p. 31.
6. L. M. Osterink and J. D. Foster, "Efficient High Power Nd:YAG Laser Characteristics", presented at 1969 IEEE Conference on Laser Engineering and Application, Washington, D.C., May 1969; W. Koechner, "Multi-hundred Nd:YAG CW Laser", Contribution TuE12, 1969 Annual Meeting of Optical Soc. of Amer.
7. K. Schmidt, "Radiation Characteristics of High Pressure Alkali Metal Discharges", Proc. 6th International Conf. on Ionization Phenomena in Gases (Paris 1963), Vol. 3, pp 323-330.
8. R. Stair, R. G. Johnston, and E. W. Halbach, "Standards of Spectral Radiance for the Region of 0.25 to 2.6 Microns", J. Res. Nat'l. Bur. Standards, 64A 291 (1960); R. Stair, W. E. Schneider, and J. K. Jackson, "A New Standard of Spectral Irradiance", Applied Optics, 2, 1151 (1963).

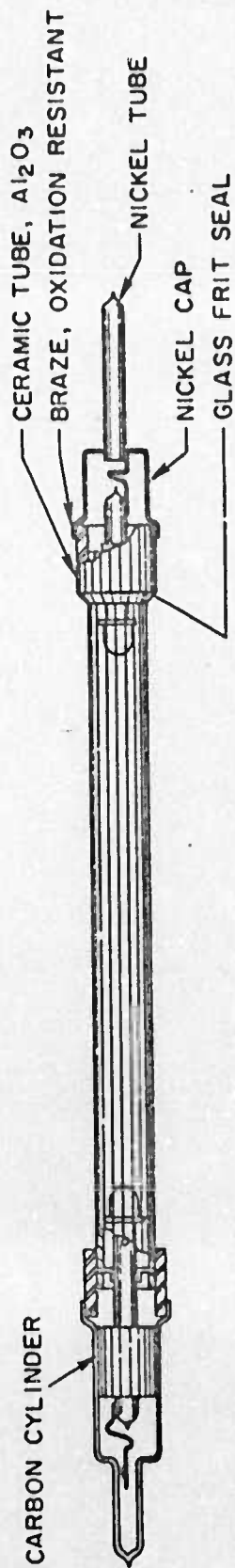


9. W. E. Forsythe and F. I. Christison, "The Absorption of Radiation From Different Sources by Water and By Body Tissue", J. Opt. Soc. Am., 20, 100-12, (1930).
10. J. Richter, "BeO Cesium Envelope Source Development", NRL Contract No. N00014-71-C-0384.
11. T. S. Jen, M. F. Hoyaux, and I. S. Frost, J. Quant. Spectrosc., Radiat. Transfer, 9 487 (1969).
12. S. Yoshikawa, K. Iwamoto and K. Washio, "Efficient Arc Lamps for Optical Pumping Neodymium Lasers", App. Opt., 10, 1620 (1970).
13. J. J. Lowke, J. Quant. Spectrosc. Radiat. Transfer, 9, 839 (1969).

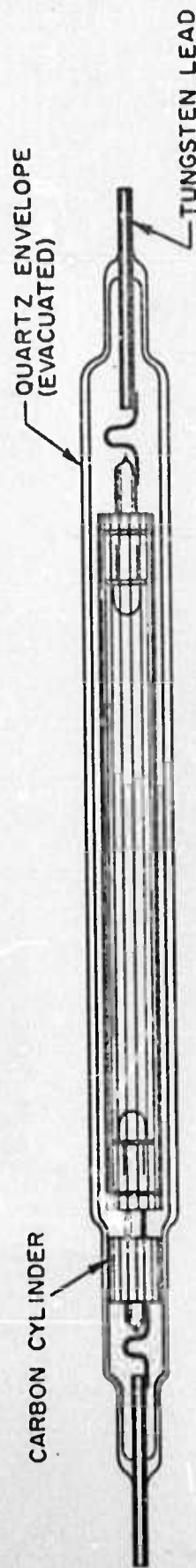




(a) BASIC ALKALI METAL LAMP - FOR USE IN VACUUM



(b) "NUDE" TUBE DESIGN - FOR USE IN AIR



(c) QUARTZ ENVELOPE - FOR USE IN AIR OR LIQUID

FIGURE 1 ALKALI METAL LAMP CONFIGURATIONS

4258



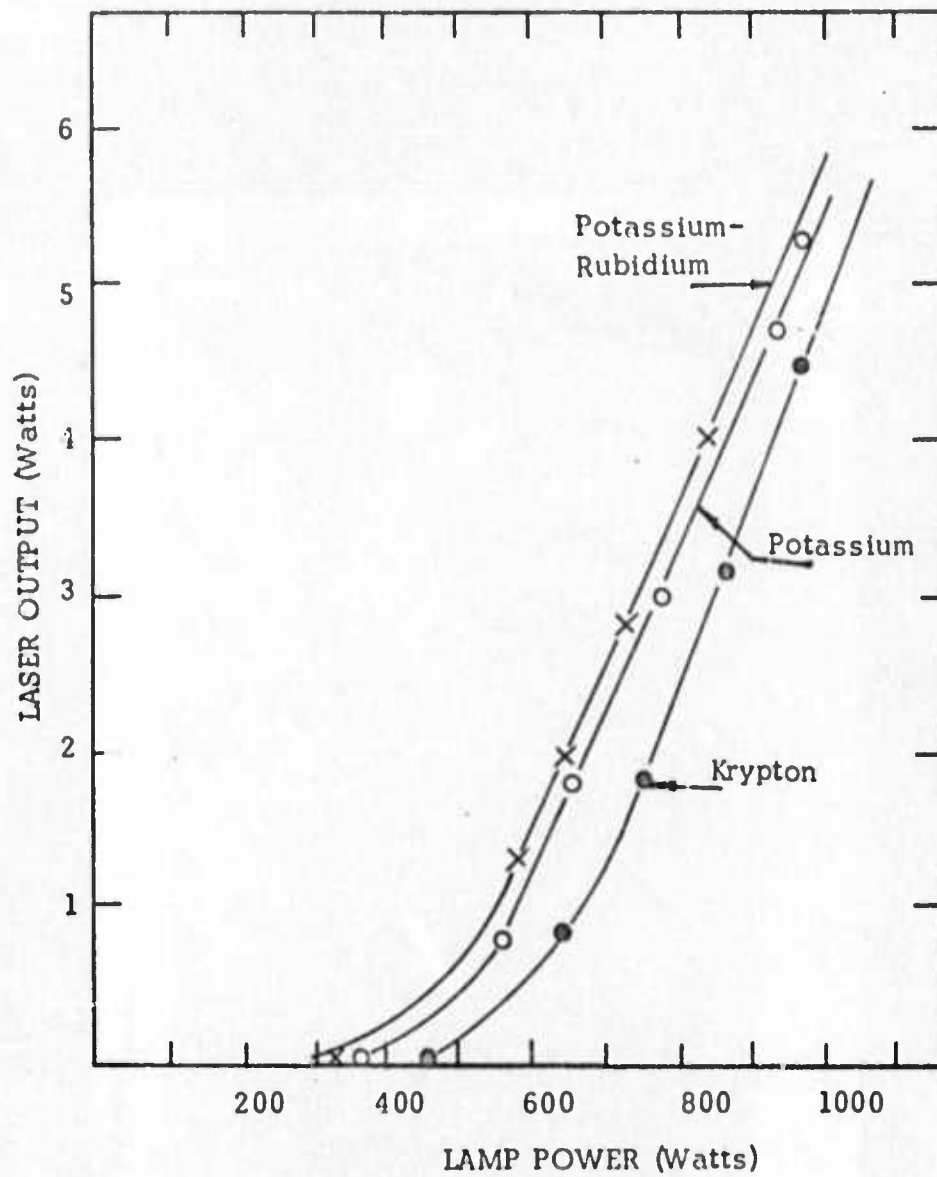


FIGURE 2 LASER DATA FOR ALKALI VAPOR LAMPS AND A KRYPTON ARC LAMP.



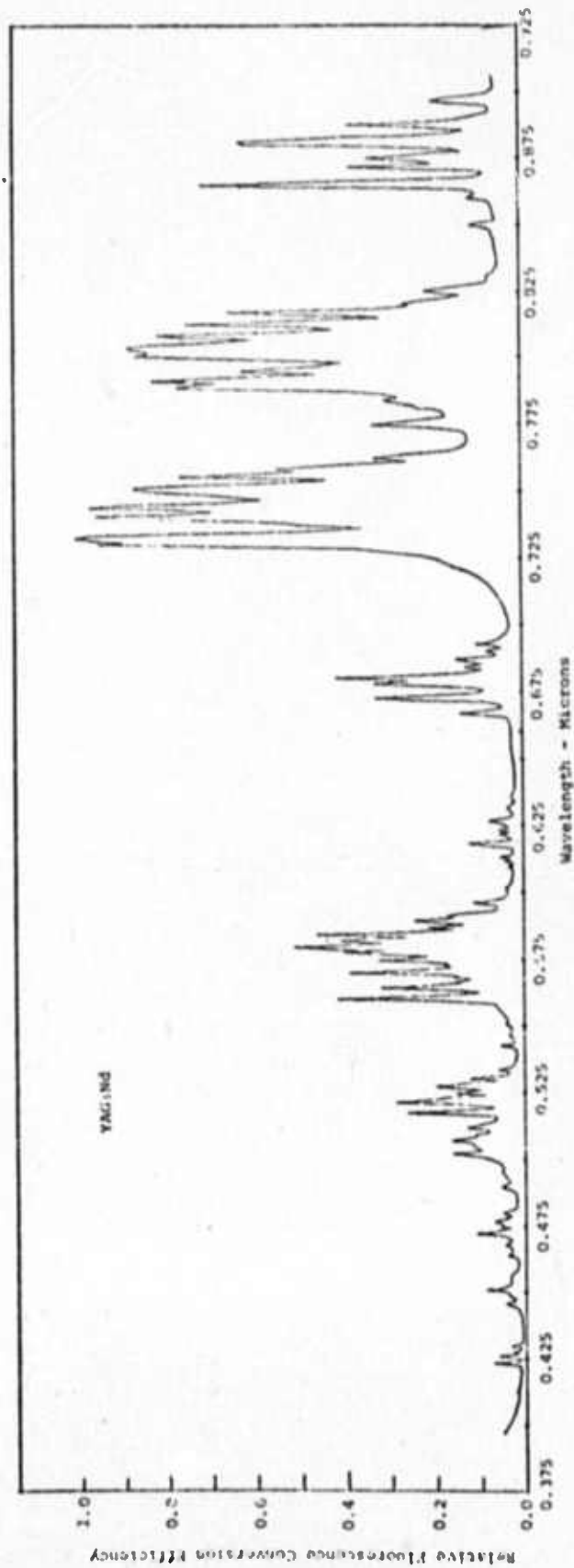


FIGURE 3 EXCITATION SPECTRA FOR Nd:YAG



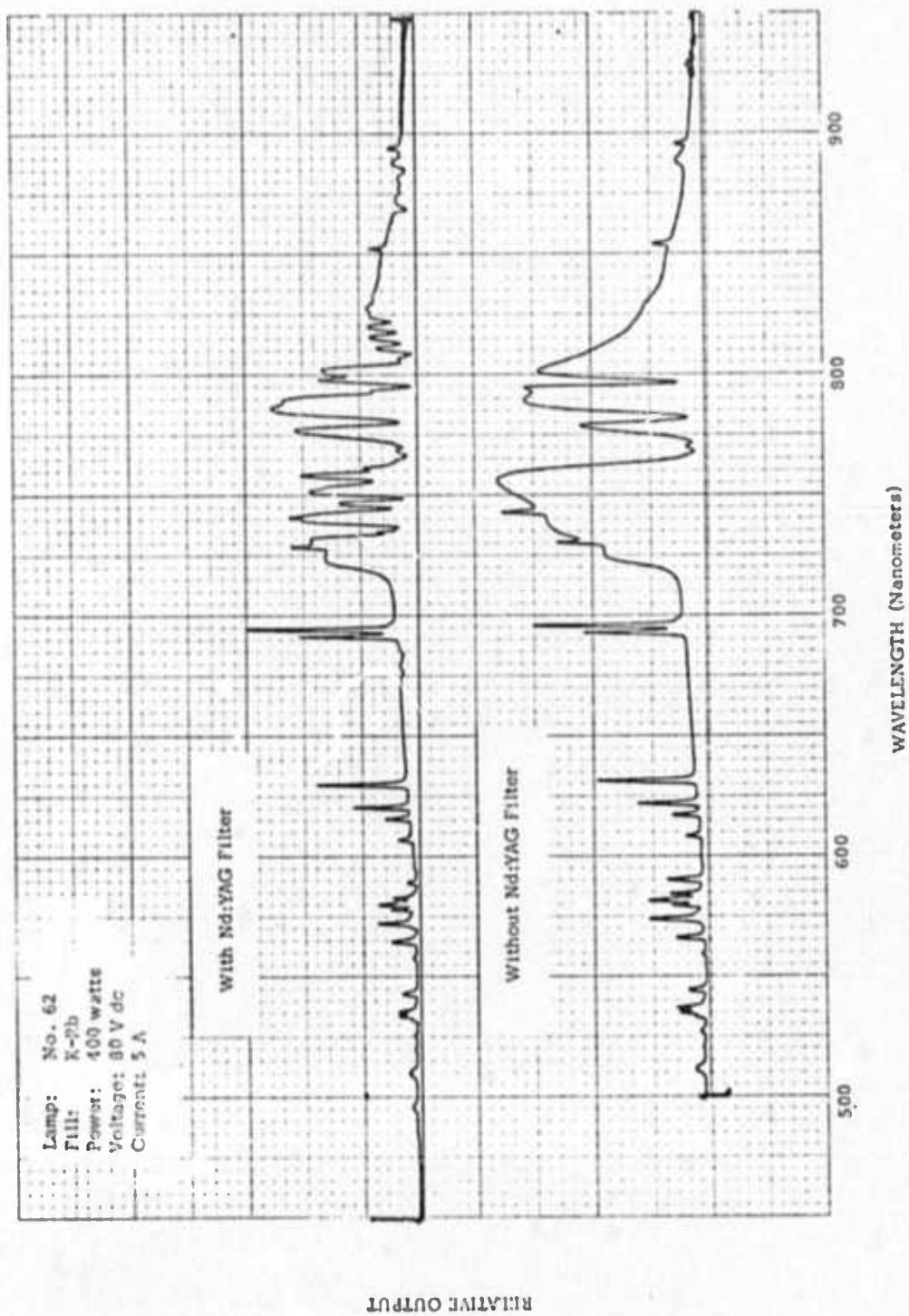
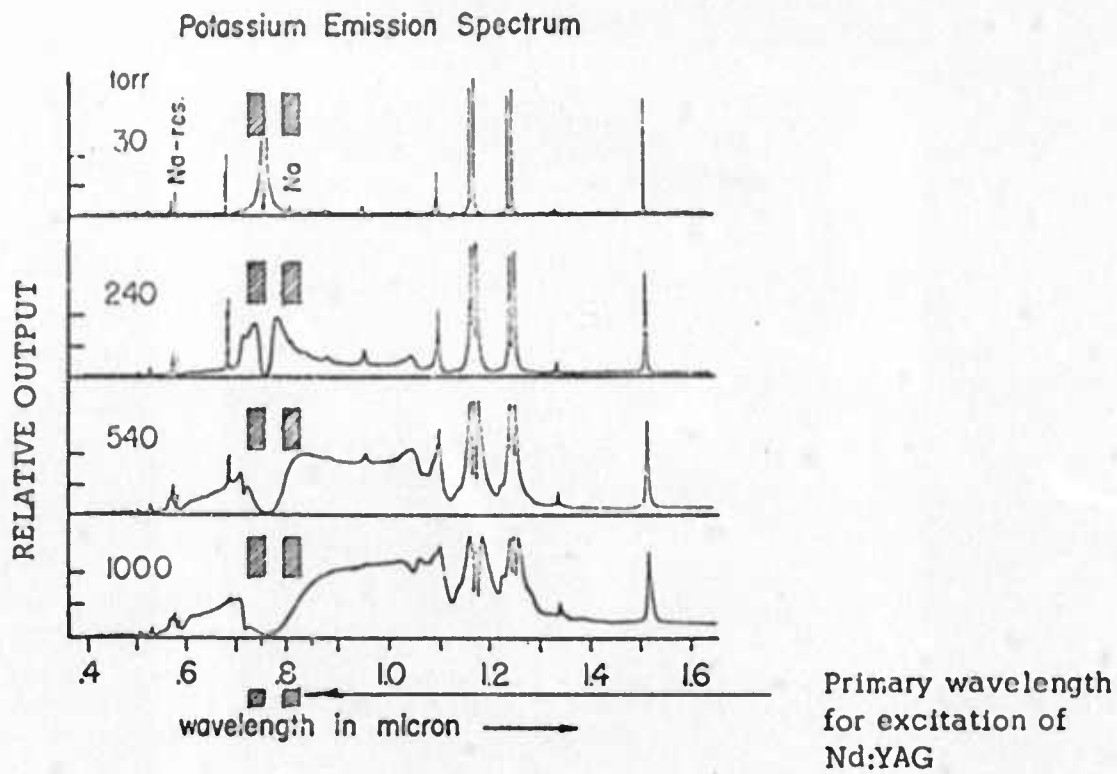


FIGURE 4. SPECTRUM FROM ALKALI VAPOR LAMP AT OPTIMUM PRESSURE

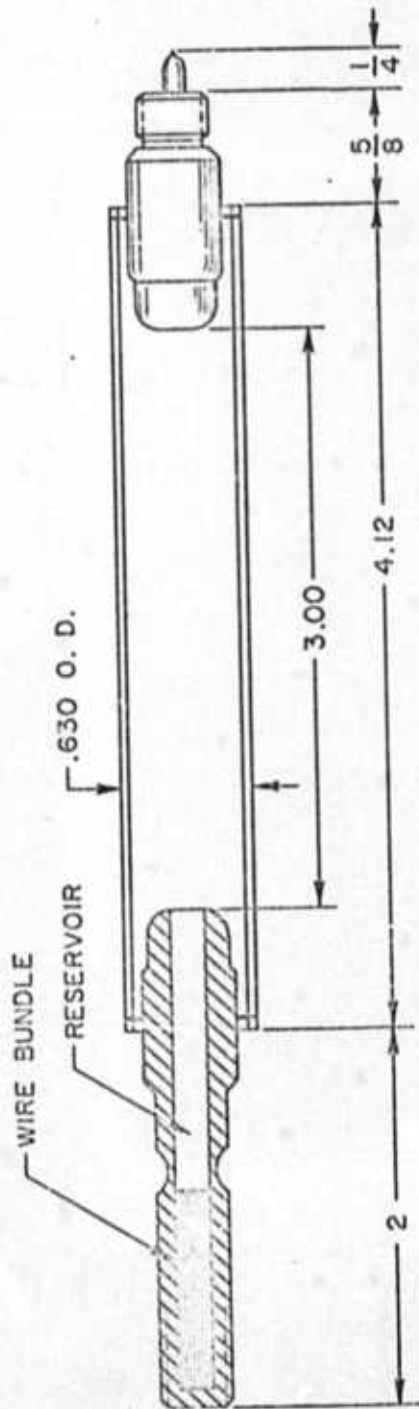




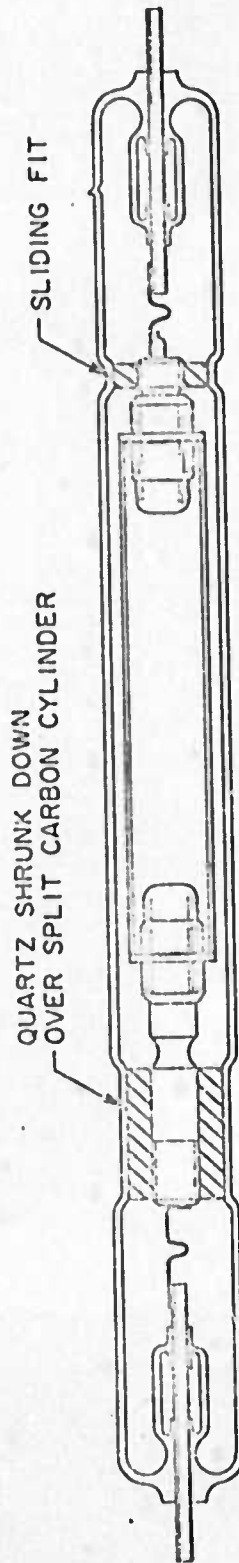
Source: Reference 7

FIGURE 5 POTASSIUM EMISSION SPECTRUM AS A FUNCTION OF PRESSURE





ALKALI METAL LAMP, 14.5 mm BORE DIAMETER



ALKALI METAL LAMP, 14.5 mm BORE DIAMETER, IN QUARTZ JACKET

FIGURE 6 ALKALI VAPOR LAMP; 14.5 MM BORE DIAMETER



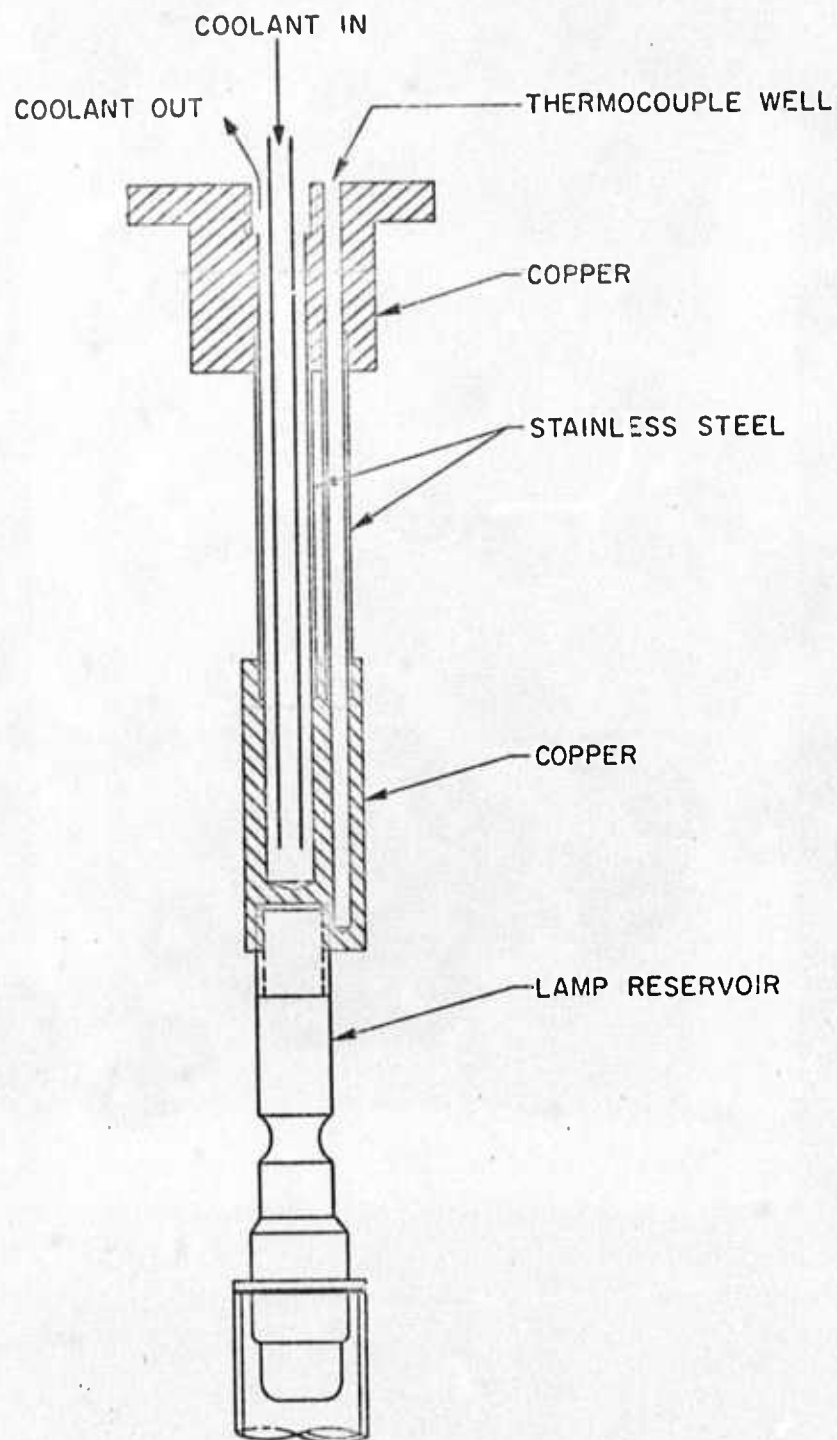


FIGURE 7 MOUNTING FIXTURE FOR CONTROLLING RESERVOIR TEMPERATURE OF ALKALI VAPOR ARC LAMP



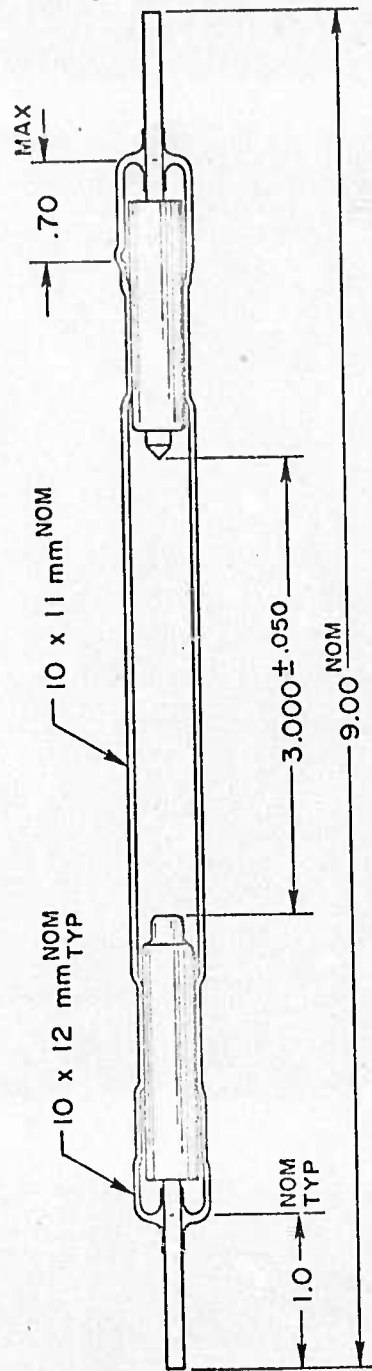
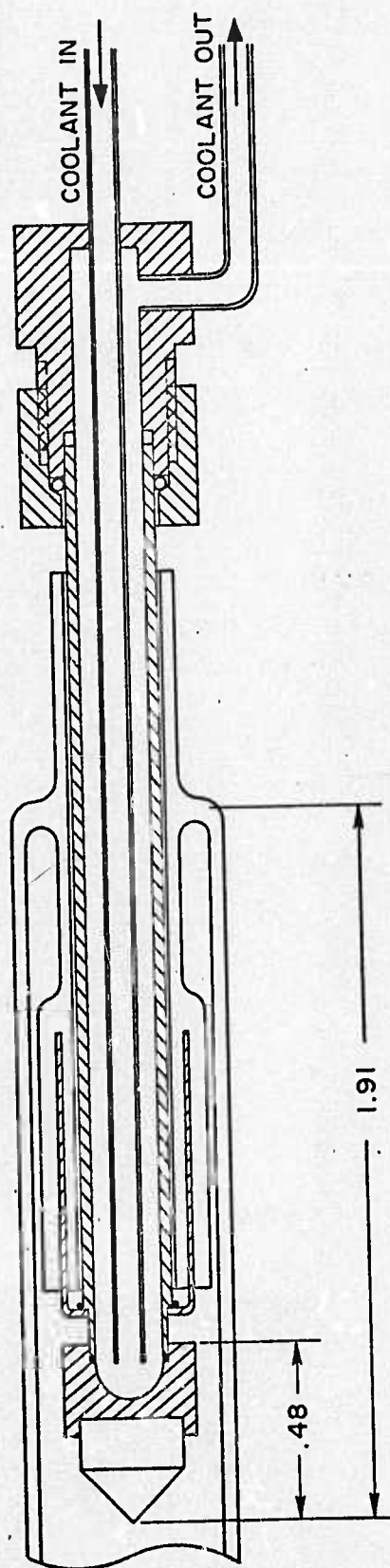
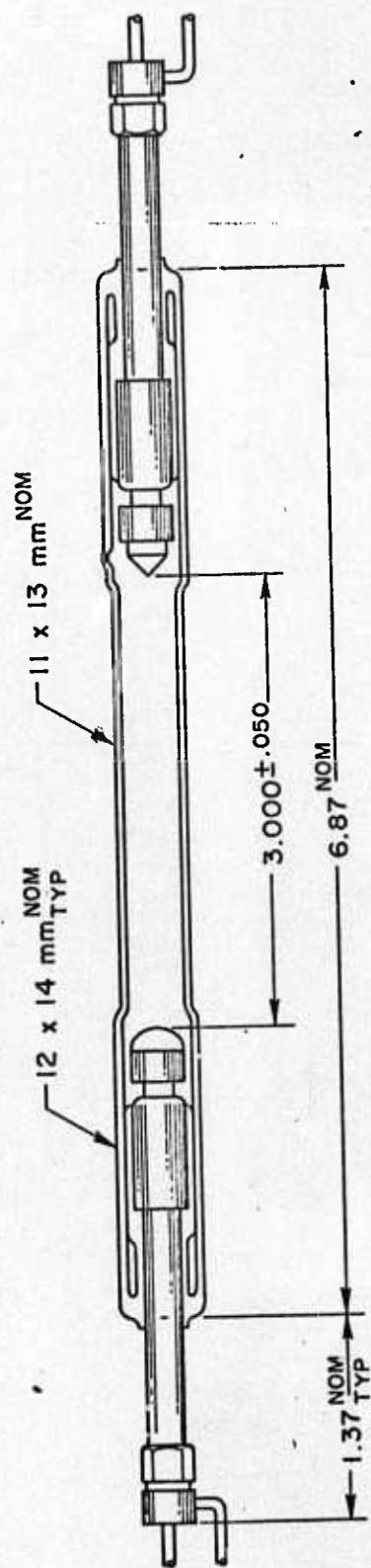


FIGURE 8 KRYPTON ARC LAMP WITH EXTERNALLY WATER COOLED ELECTRODES





DETAIL, INTERNAL COOLANT PASSAGES

FIGURE 9 KRYPTON ARC LAMP WITH INTERNALLY WATER COOLED ELECTRODES



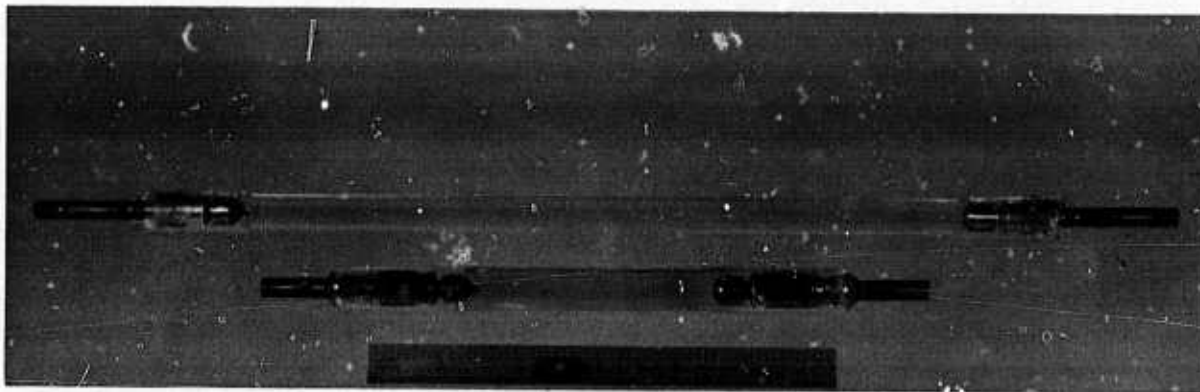


FIGURE 10 KRYPTON ARC LAMPS WITH INTERNALLY WATER COOLED  
ELECTRODES. 10 MM BORE DIAMETER, 8 kW AND 20 kW



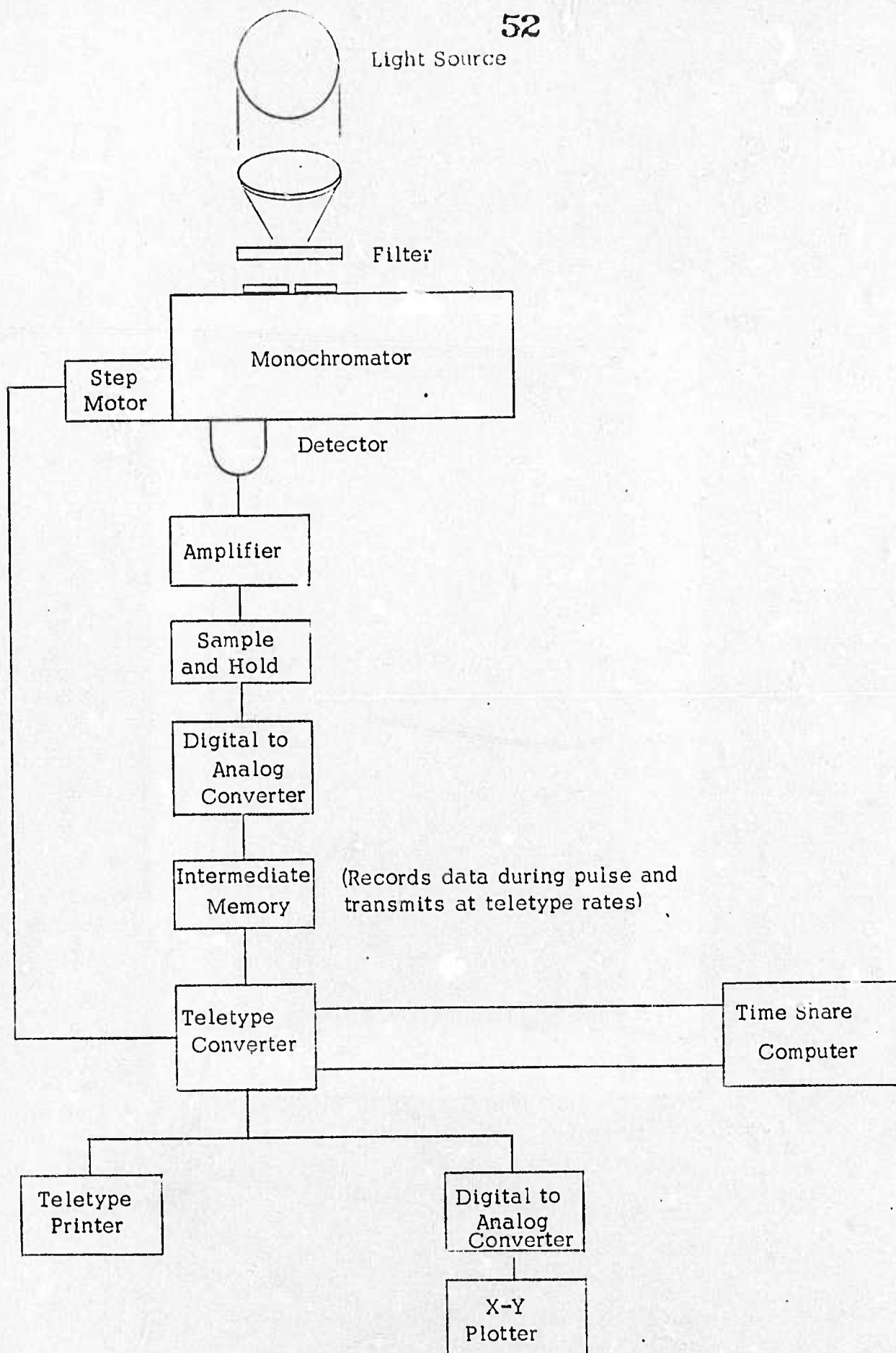


FIGURE 11 SCHEMATIC DIAGRAM OF EQUIPMENT FOR RECORDING LAMP SPECTRA



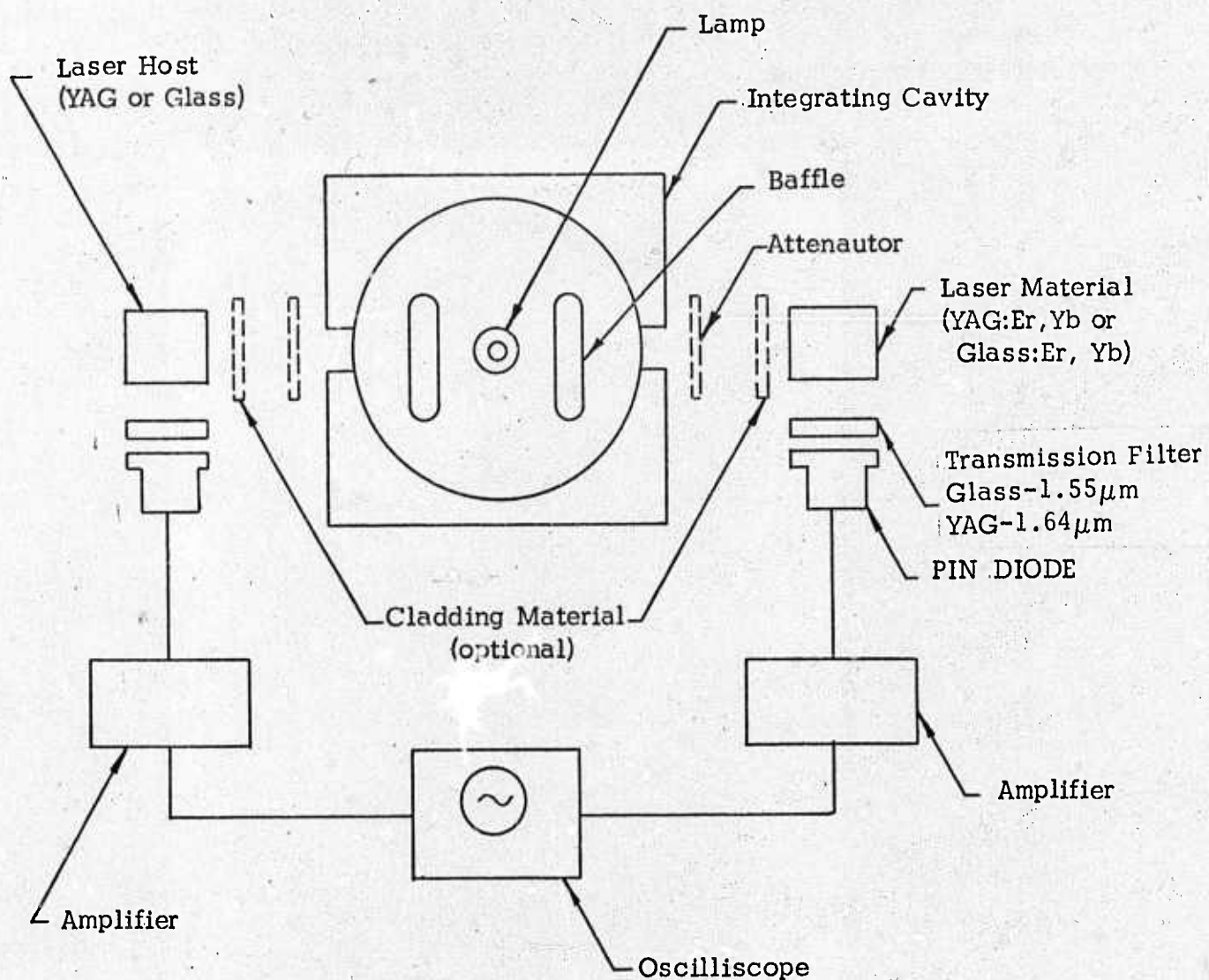
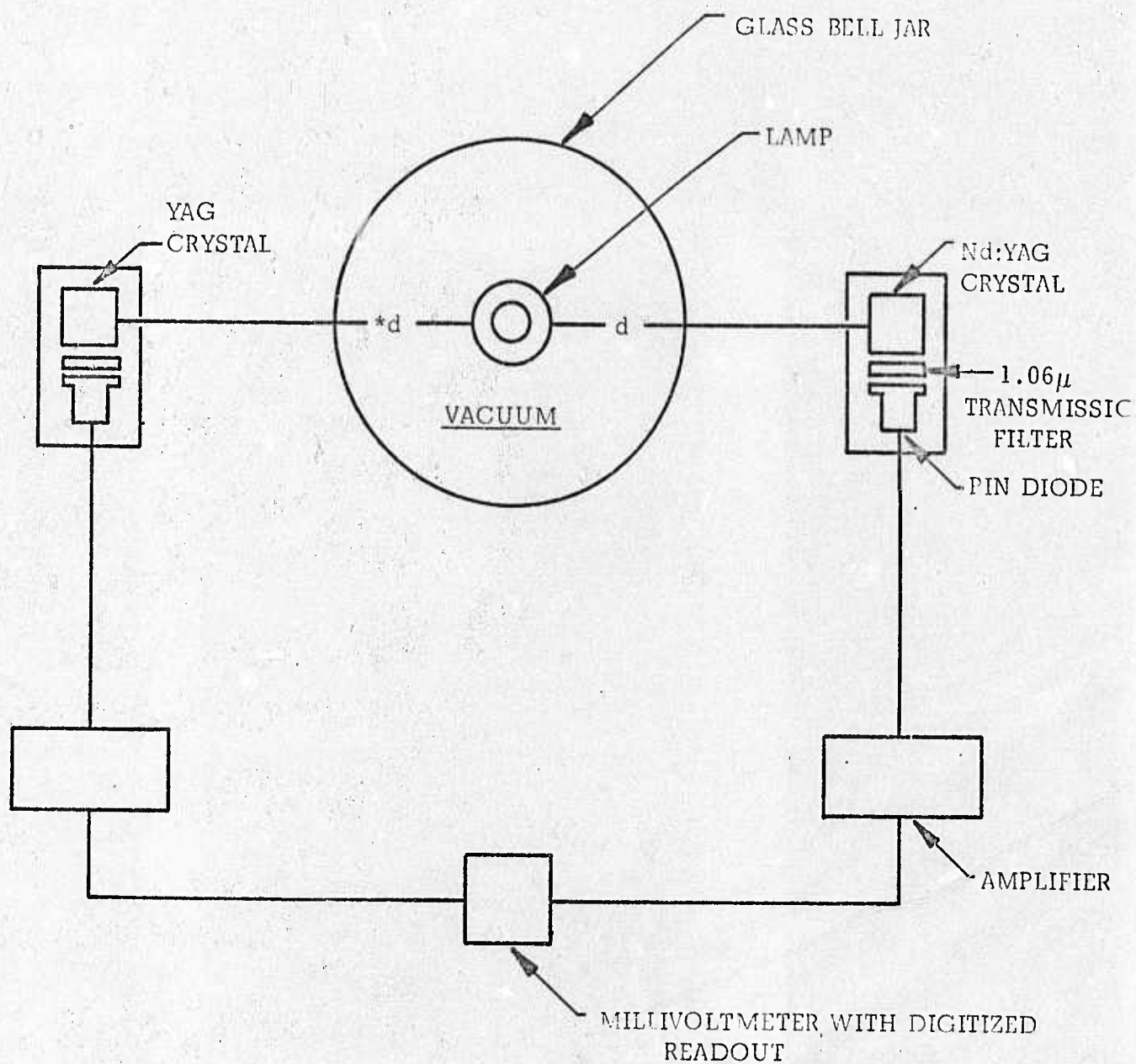


FIGURE 12 FLUORESCENCE ANALYSIS TEST DEVICE WITH LAMP MOUNTED IN INTEGRATING CAVITY





$*d$  is a fixed distance

FIGURE 13 FLUORESCENCE ANALYSIS TEST DEVICE WITH LAMP MOUNTED IN VACUUM BELL JAR



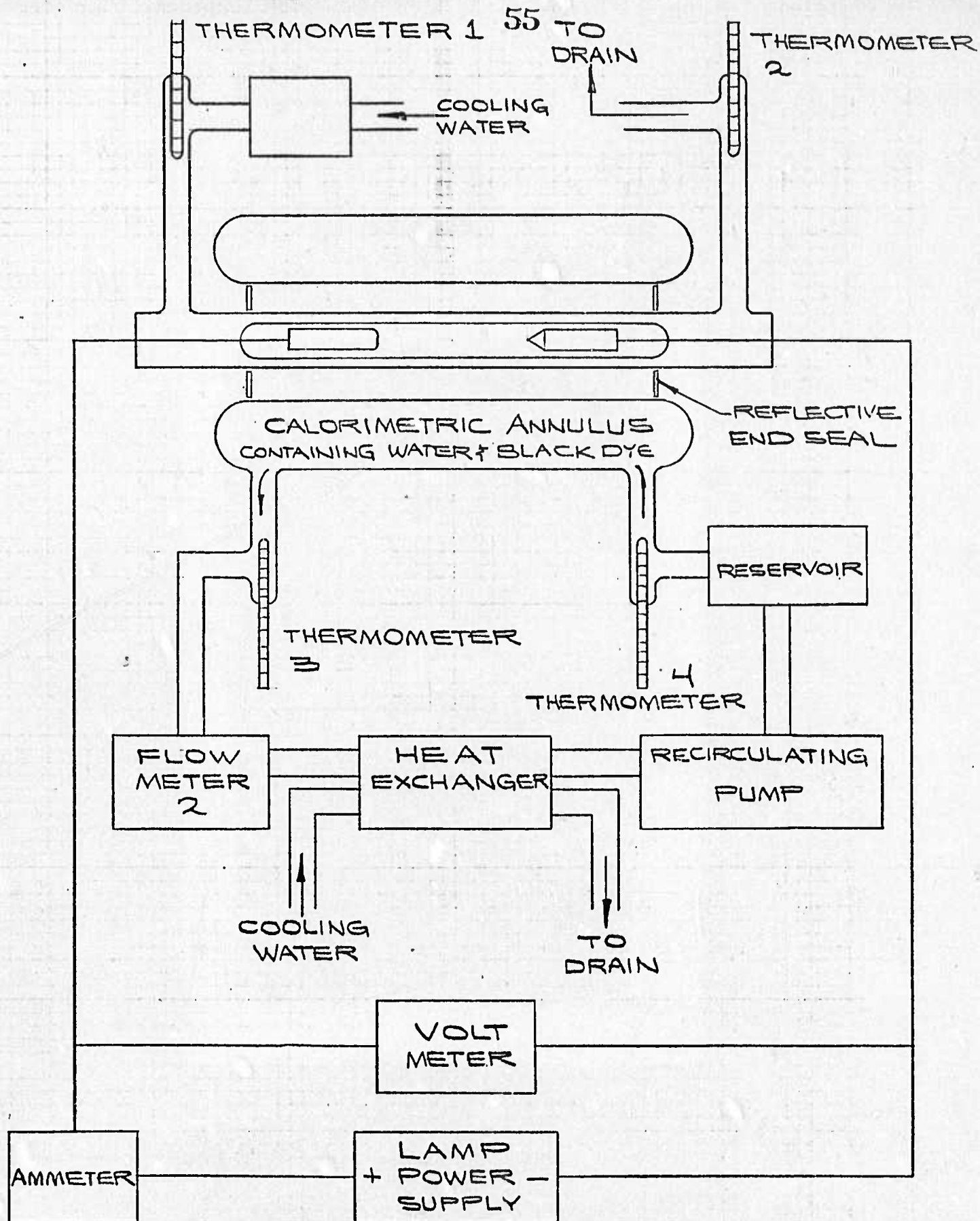
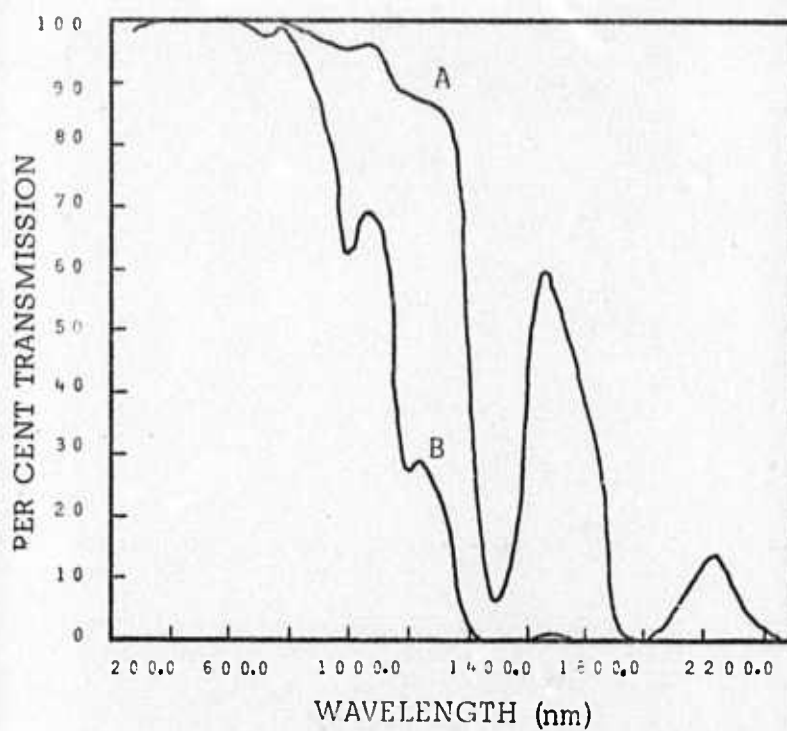


FIGURE 14 CALORIMETRIC MEASUREMENT EQUIPMENT.





Curve A, Transmission for a thickness of 1mm  
Curve B, Transmission for a thickness of 1cm

FIGURE 15 SPECTRAL TRANSMISSION OF WATER



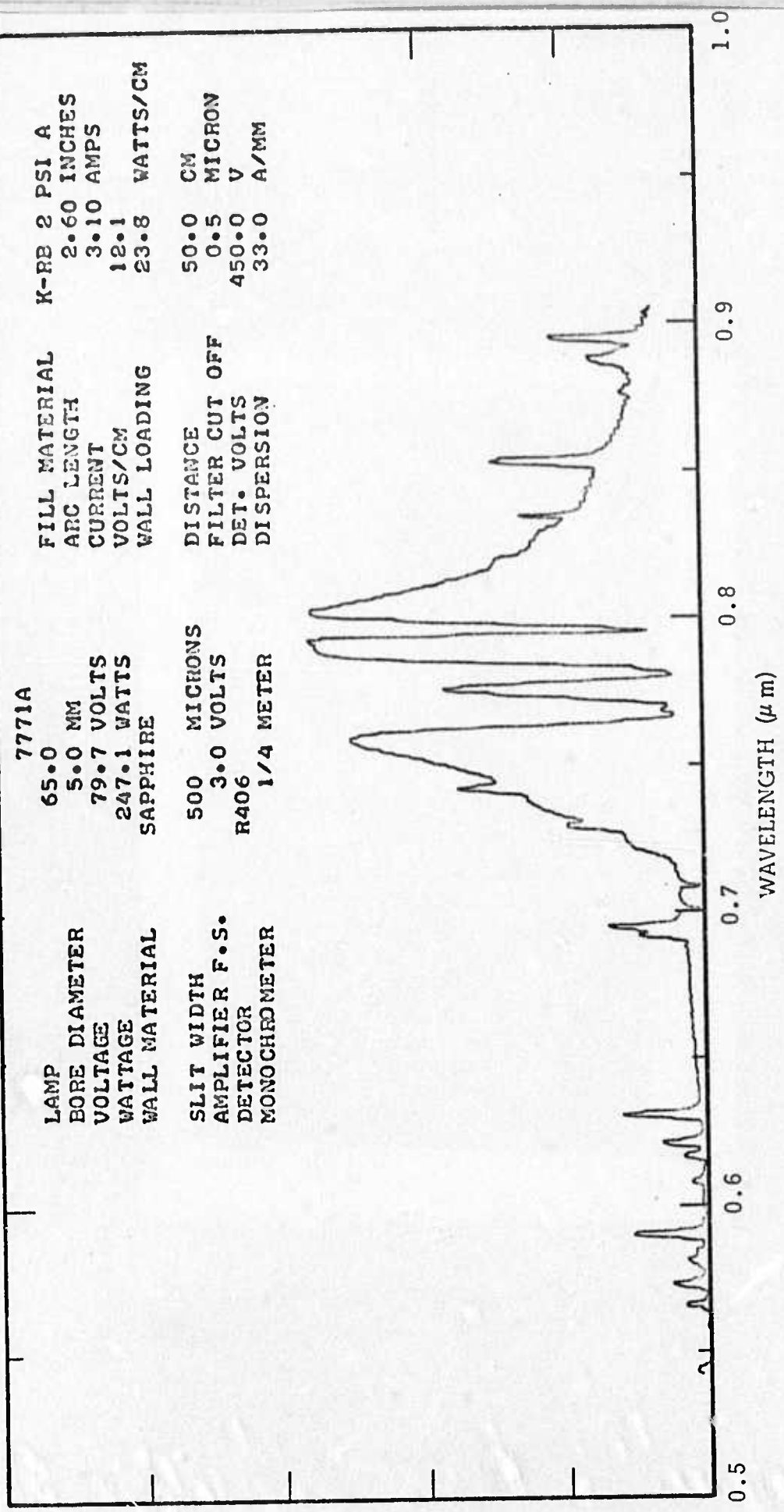


FIGURE 16 SPECTRUM OF K-Rb LAMP WITH 50 TORR OF ARGON AT OPTIMUM PRESSURE



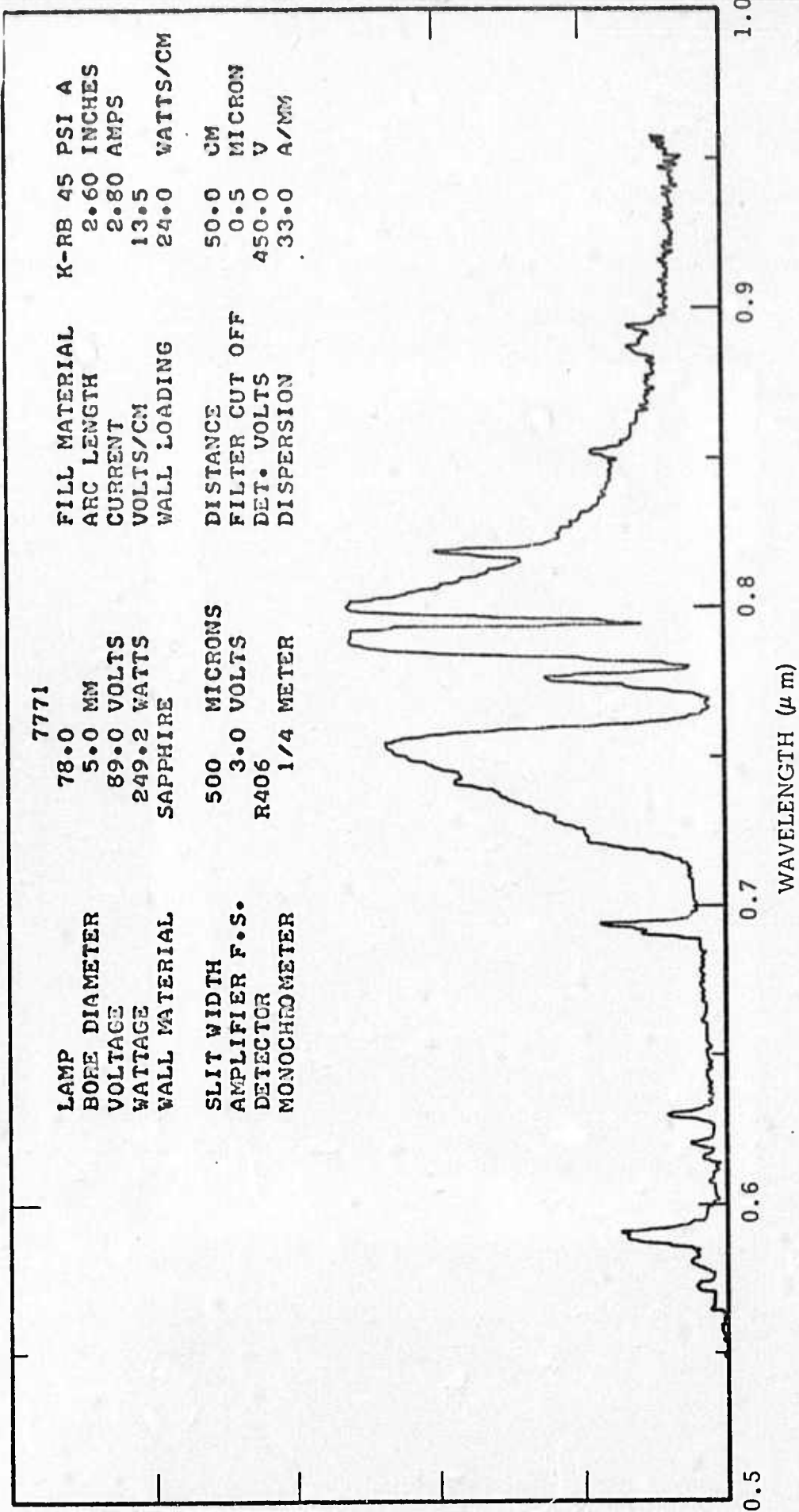
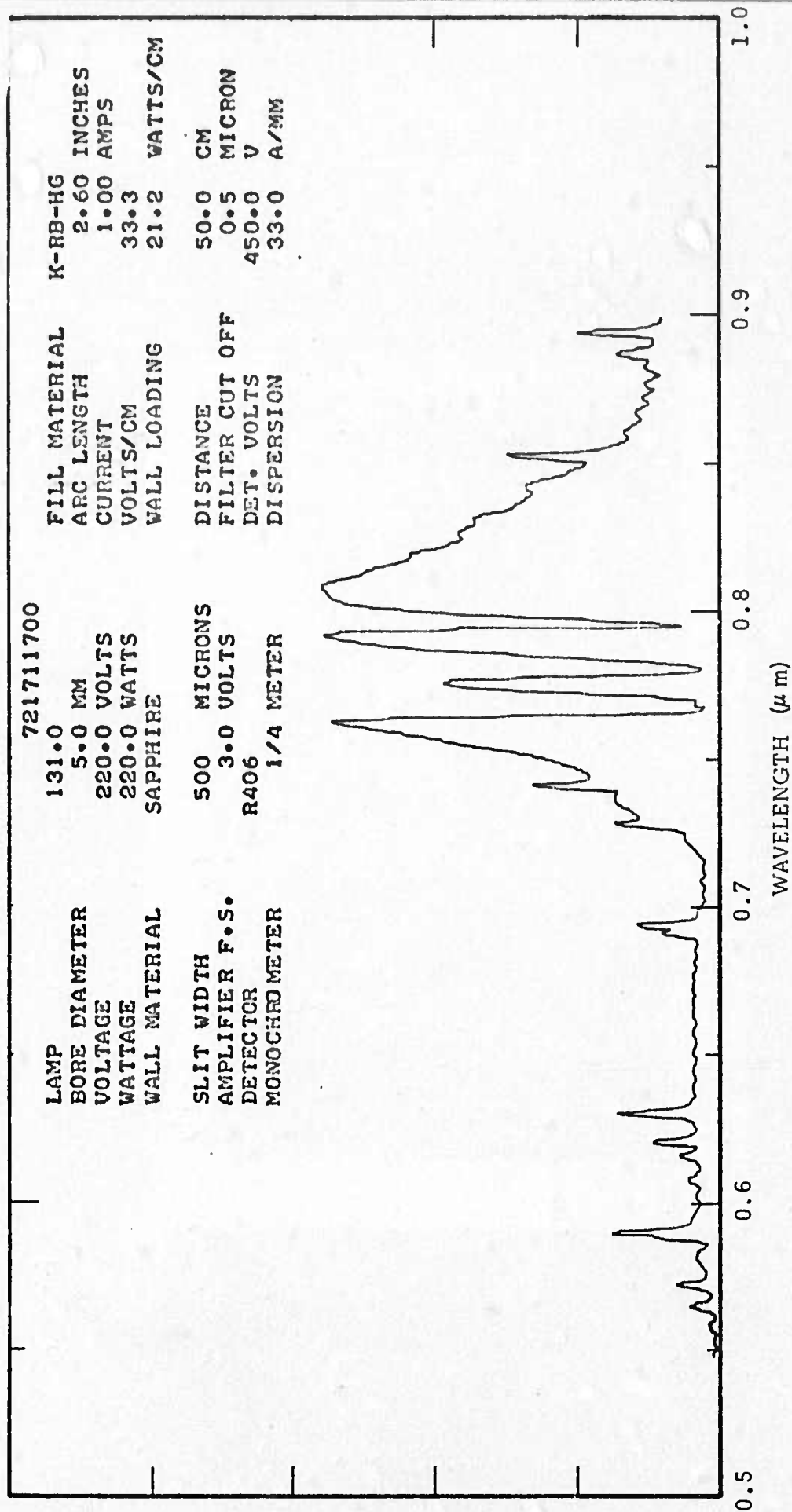


FIGURE 17 SPECTRUM OF K-Rb LAMP WITH 3000 TORR OF ARGON AT OPTIMUM PRESSURE





SPECTRAL IRRADIANCE (ARBITRARY UNITS)

FIGURE 18 SPECTRUM OF K-Rb-Hg LAMP WITH 50 TORR OF ARGON AT OPTIMUM PRESSURE



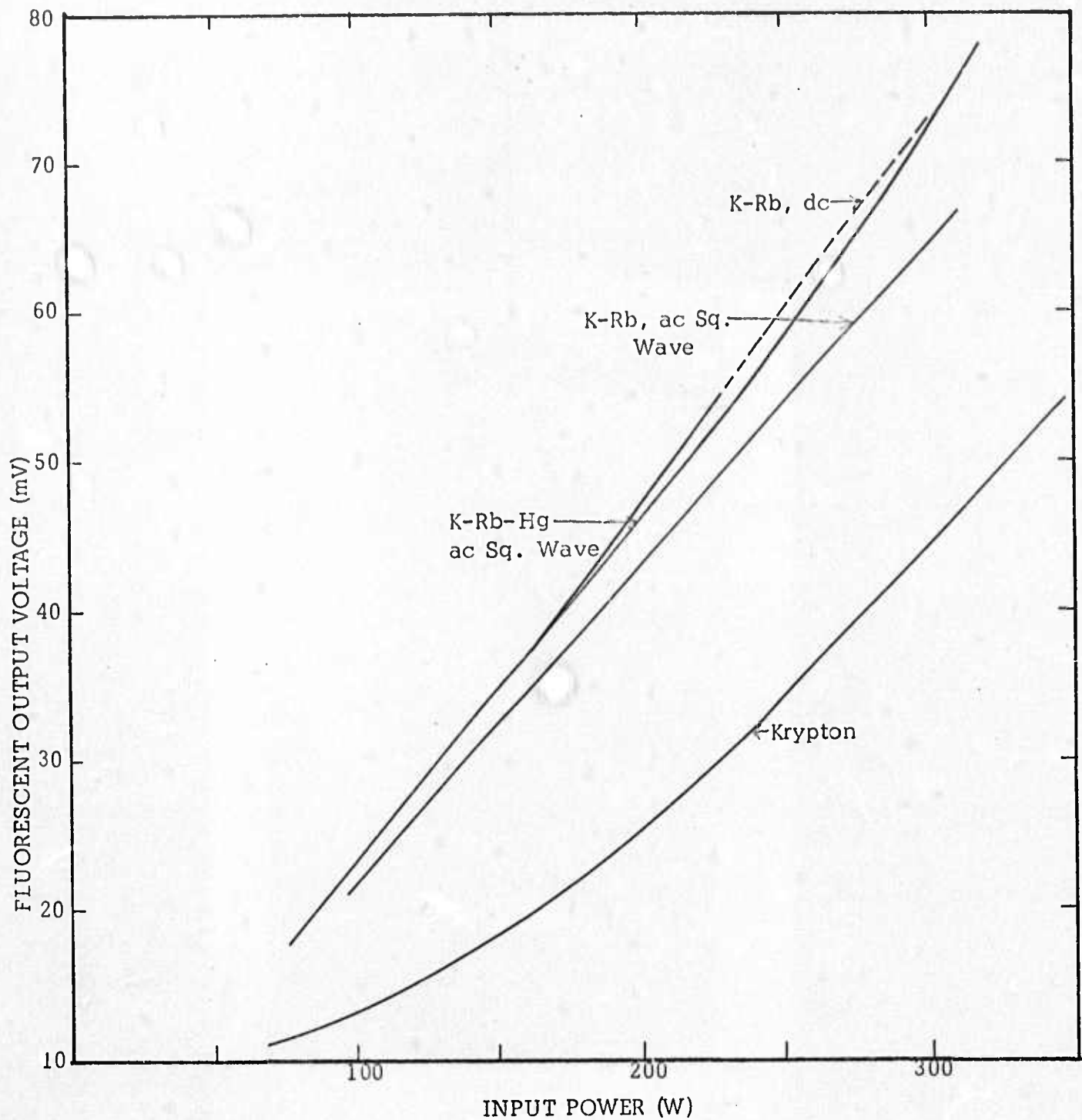


FIGURE 19 FLUORESCENCE POWER MEASUREMENTS FOR ALKALI VAPOR LAMPS AND A KRYPTON ARC LAMP (5 mm Bore, 3 Inch Arc Length)



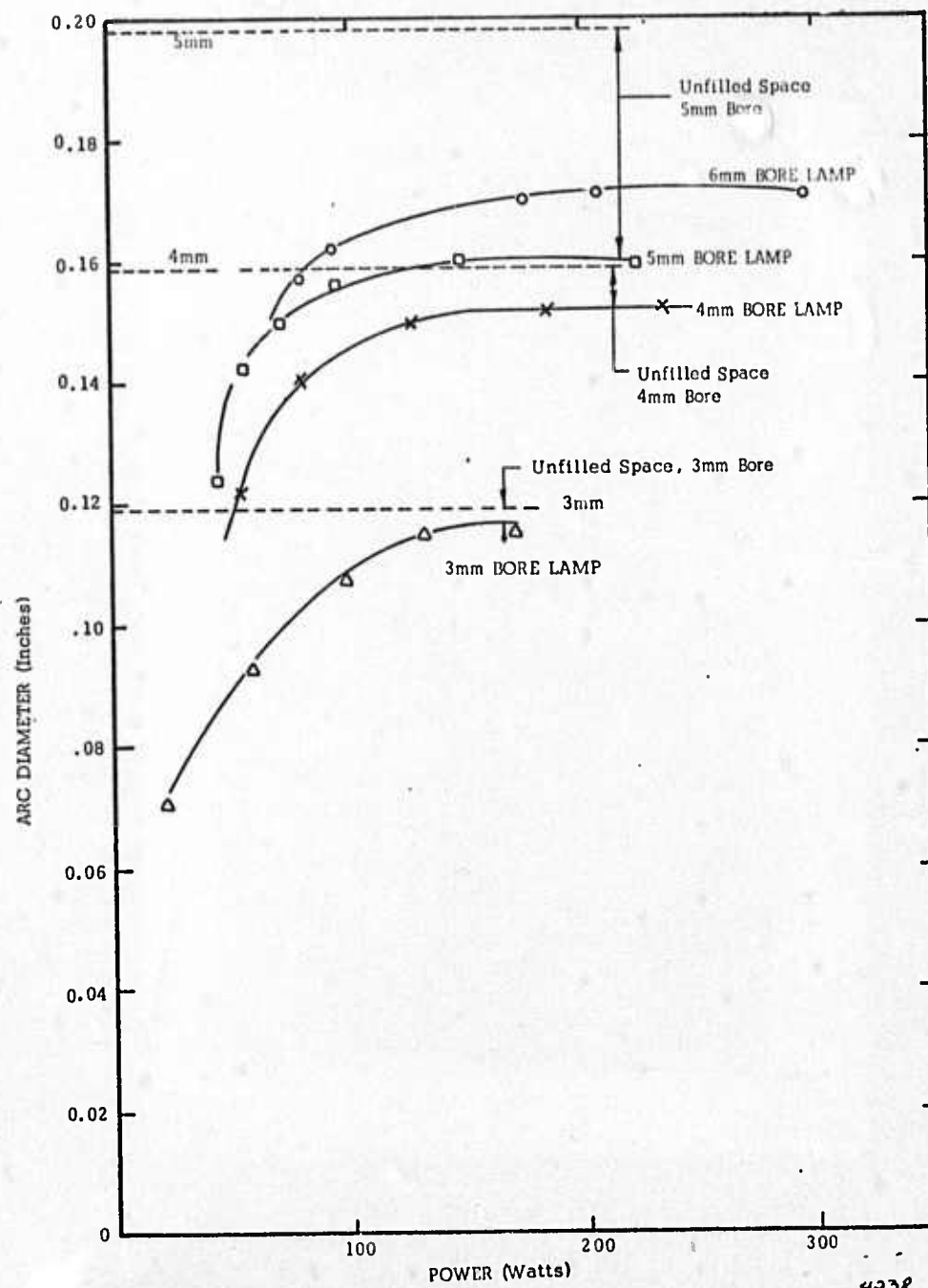


FIGURE 20 ARC DIAMETERS OF K-Rb LAMPS, 90% POINTS



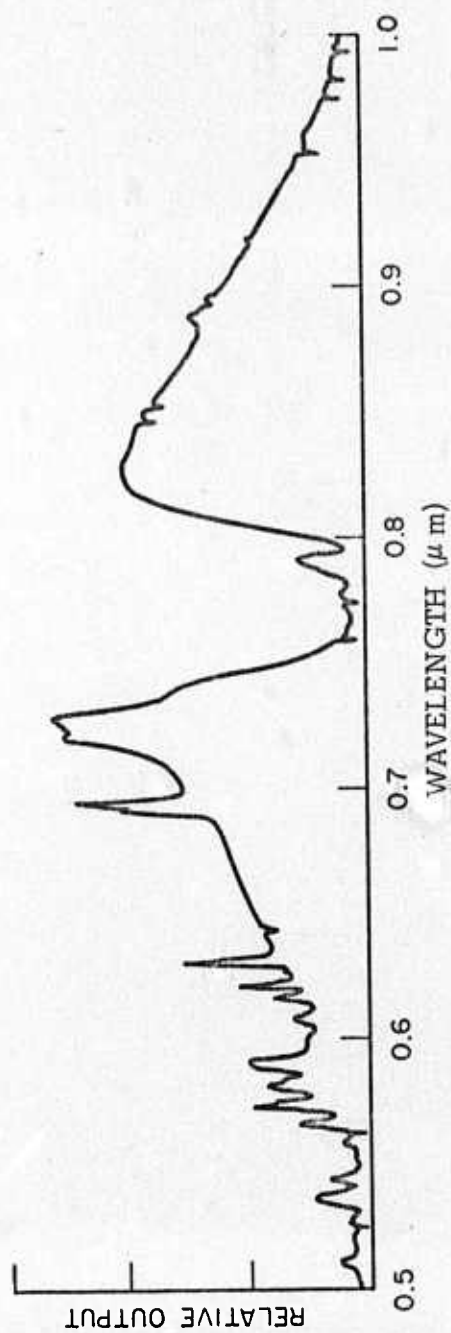


FIGURE 21 SPECTRUM OF K-Rb ARC LAMP WITH 14.5 MM BORE DIAMETER ENVELOPE,  
AT HIGH PRESSURE



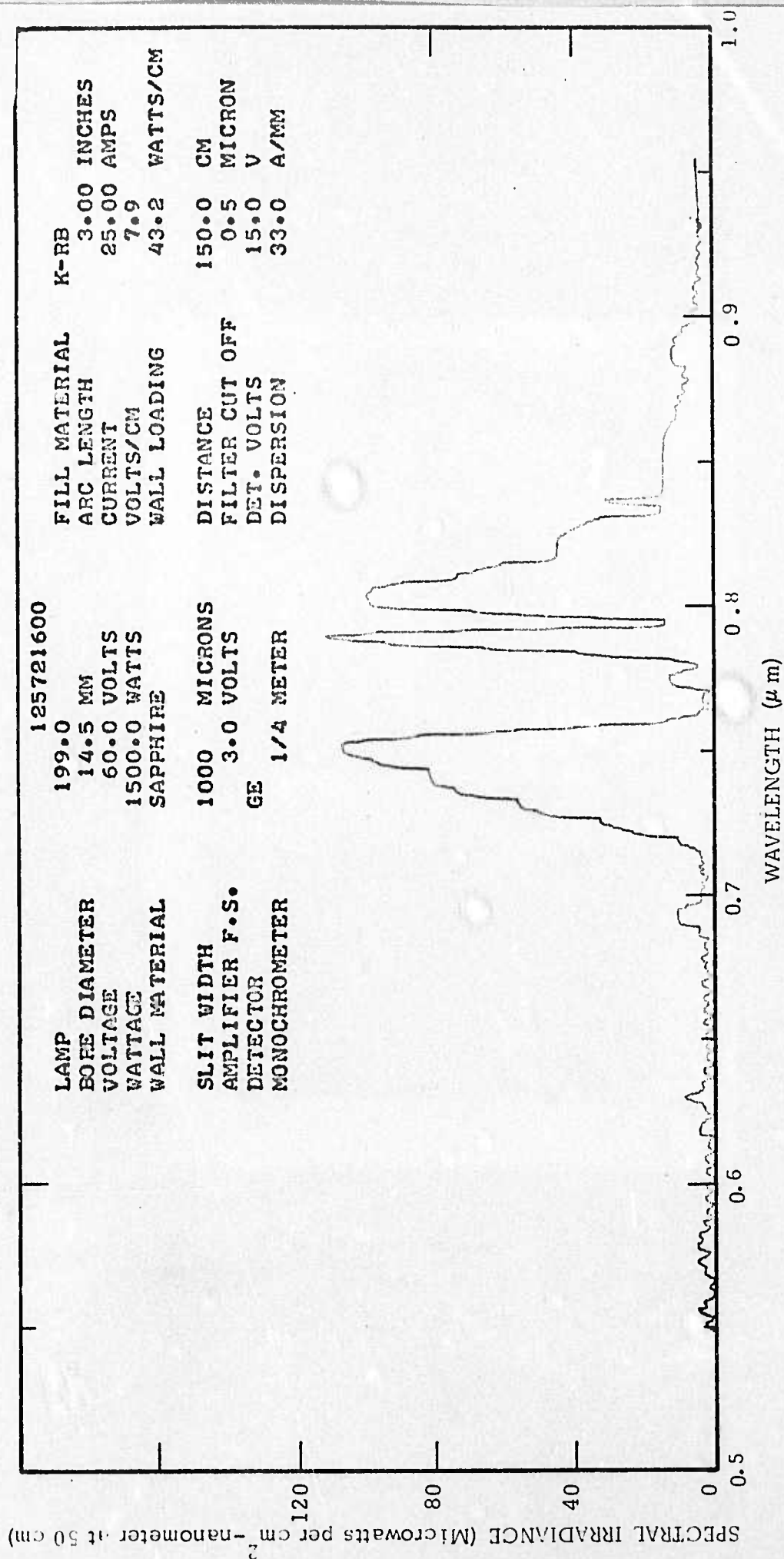


FIGURE 22 SPECTRUM OF 14.5 MM K-Rb LAMP WITH NEARLY OPTIMAL SPECTRAL MATCHING AT 1500 W/INCH INPUT POWER



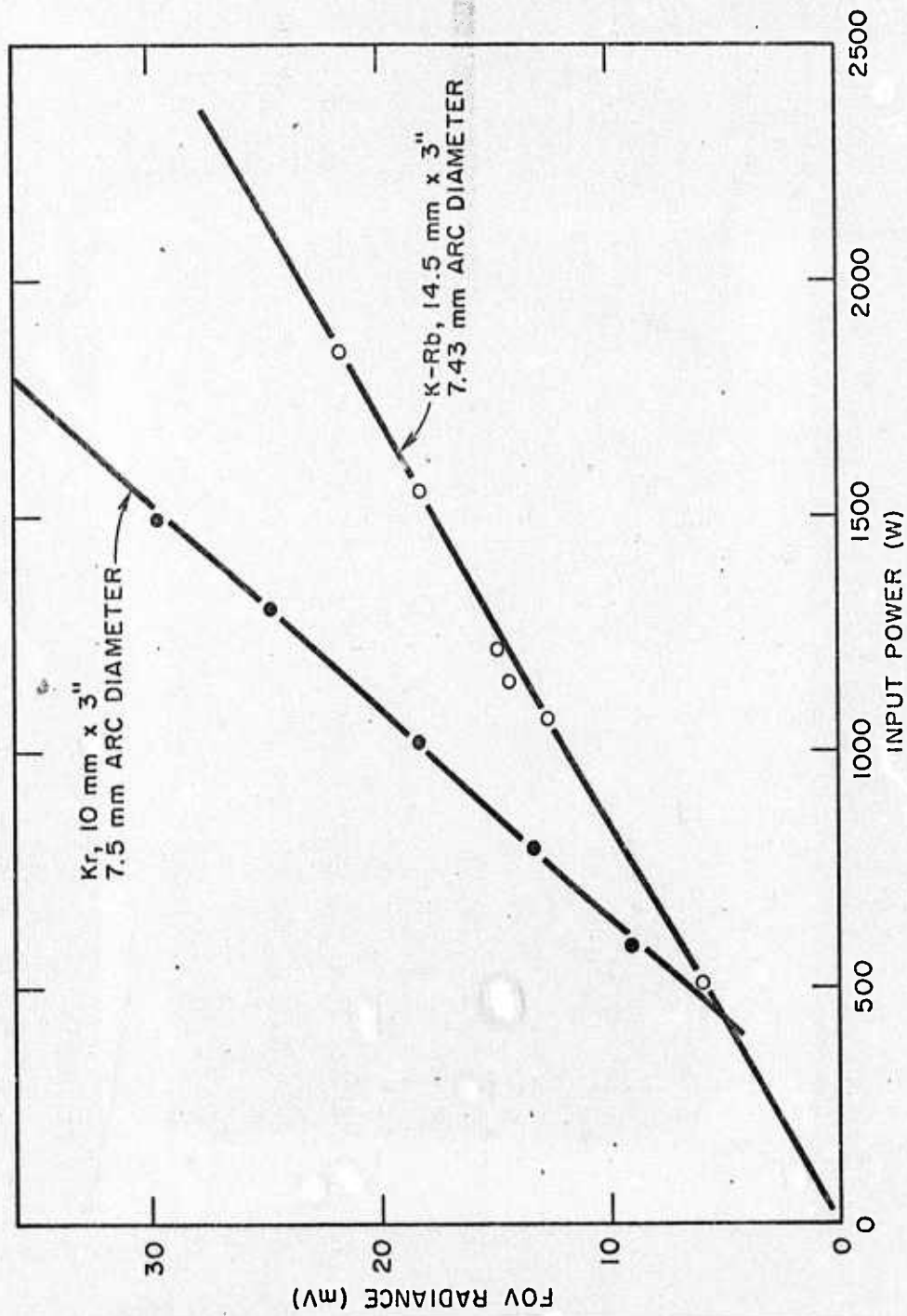


FIGURE 23 USEFUL RADIANCE OF K-Rb AND KRYPTON ARC LAMPS



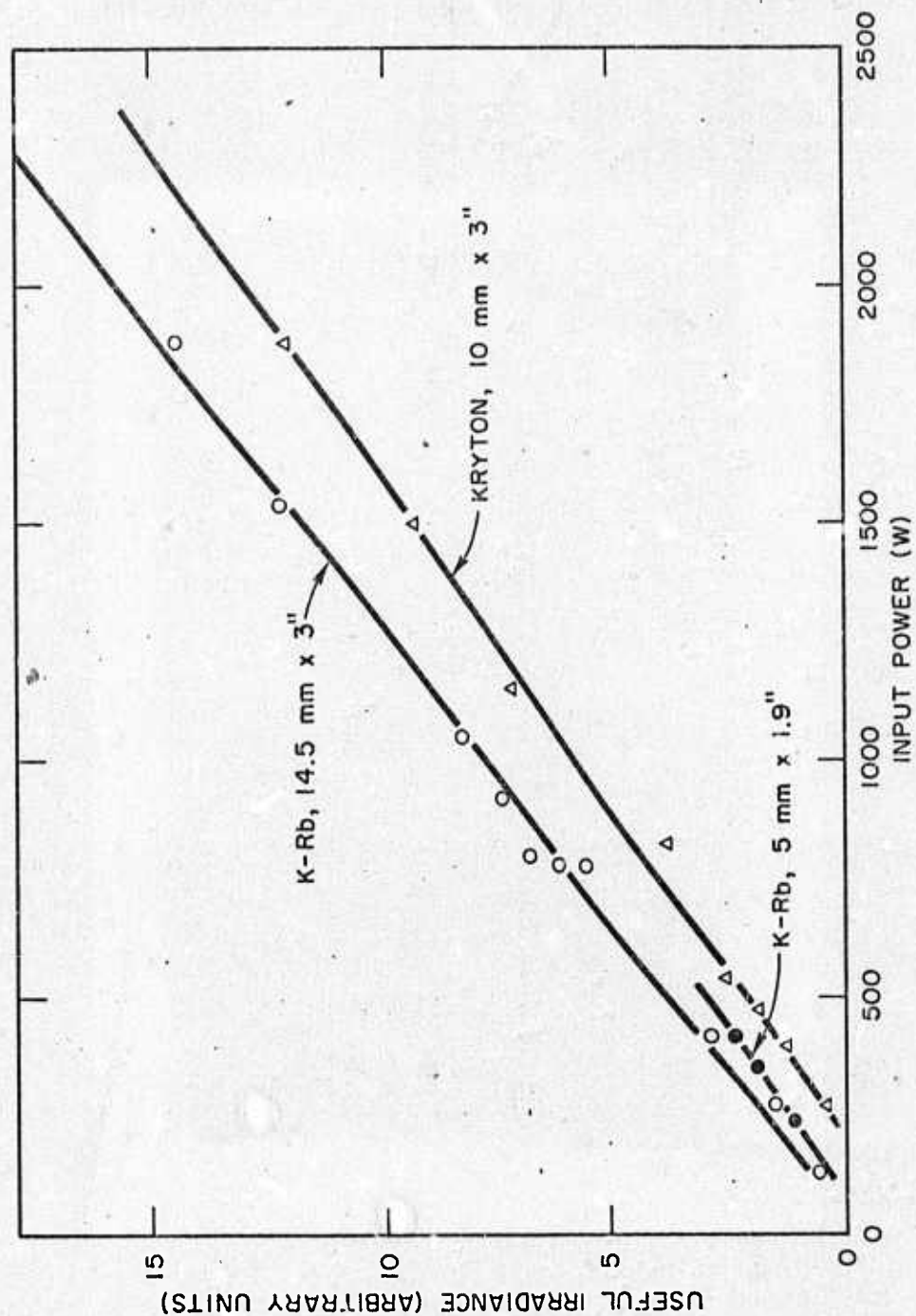


FIGURE 24 USEFUL IRRADIANCE OF K-Rb AND KRYPTON ARC LAMPS



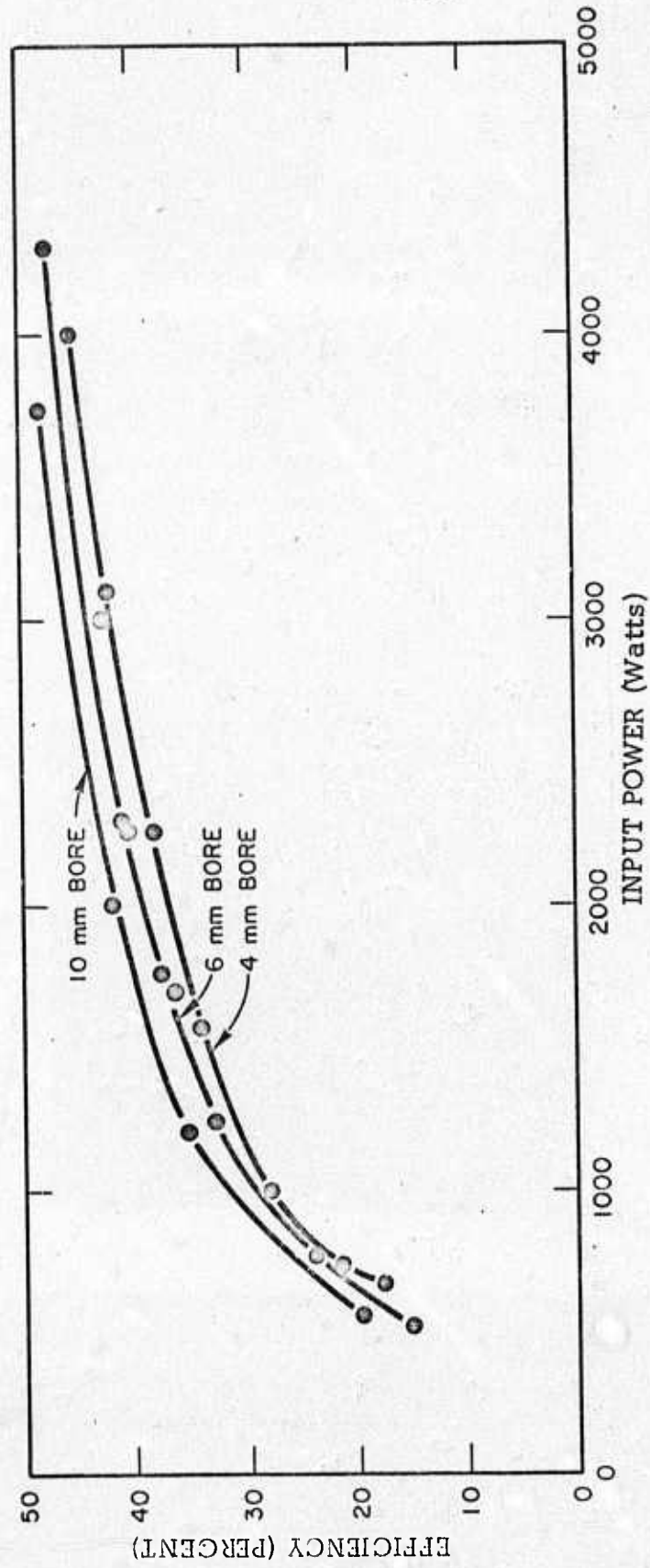


FIGURE 25 KRYPTON ARC LAMP RADIATIVE EFFICIENCY AS A FUNCTION OF INPUT POWER



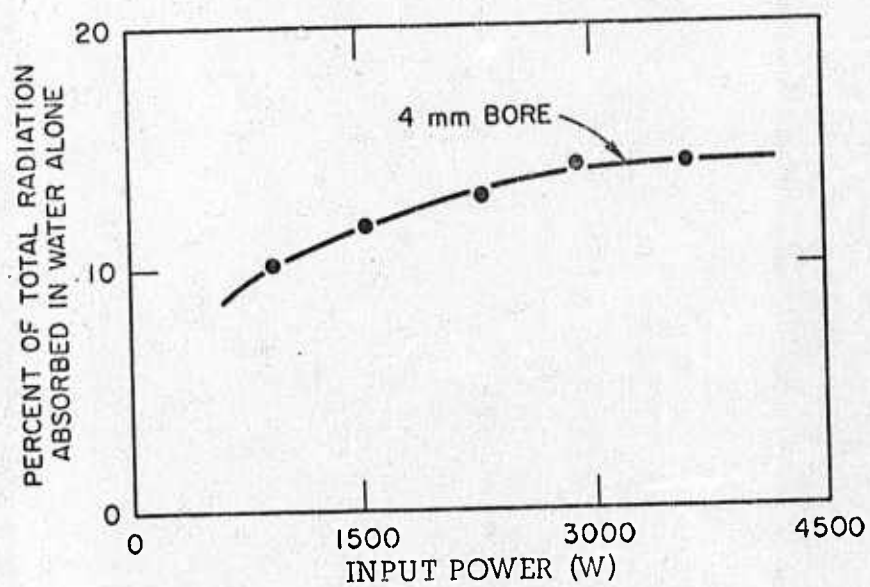


FIGURE 26 PERCENTAGE OF RADIATION FROM 4mm BORE KRYPTON ARC LAMP ABSORBED BY 6mm LAYER OF WATER



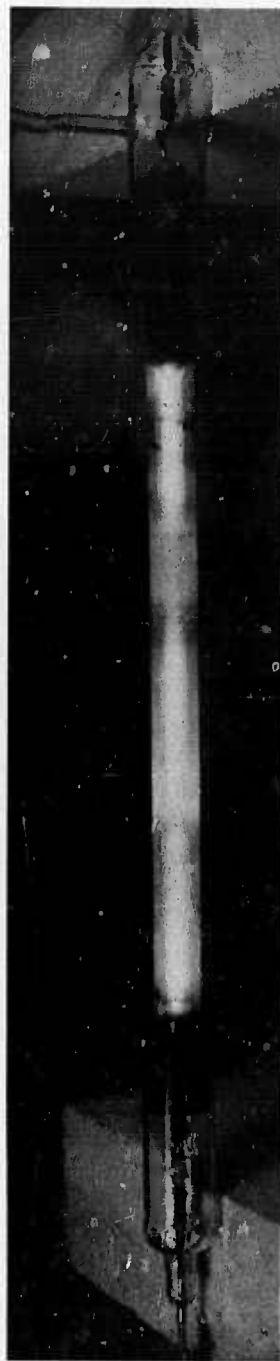


FIGURE 27 DELIVERED ITEM. K-Rb LAMP IN SAPPHIRE ENVELOPE WITH OUTER QUARTZ JACKET, 14.5 MM BORE DIAMETER, 8 INCH ARC LENGTH (LAMP OPERATING AT LOW CURRENT DURING BAKEOUT OF QUARTZ JACKET)



APPENDIX I  
RADIATIVE TRANSFER IN RESONANCE RADIATION  
DOMINATED PLASMAS



# RADIATIVE TRANSFER IN RESONANCE RADIATION DOMINATED PLASMAS

The intensity of a beam of light travelling in the positive  $x$  direction is given by the equation<sup>(1)</sup>

$$I_+(x, \omega) = \int_{-R}^x k(x', \omega) B(x', \omega) e^{-(t-t')} dx' \quad (1)$$

where  $I_+(x, \omega)$  is the intensity in terms of power per unit area, per unit angular frequency interval, and per steradian;  $k(x, \omega)$  is the absorption coefficient,  $B(x, \omega)$  is the Planck function,  $8\pi^2\omega^2 h / (e^{2\pi h\omega/kT} - 1)$  and  $t(x, \omega)$  is the optical thickness at  $x$ , defined by

$$t(x, \omega) = \int_{-R}^x k(x'', \omega) dx'' \quad (2)$$

In Equations (1) and (2) the lower limit of the integral,  $-R$ , is the co-ordinate of the boundary of the plasma in the negative  $x$  direction. The intensity is assumed to be zero at  $-R$ .

For a Lorentzian shaped line,

$$k(x, \omega) = \frac{k_0(x) W(x)}{\pi (W(x)^2 + \Delta\omega^2)} \quad (3)$$

where  $k_0(x)$  is the integrated absorption coefficient,  $\Delta\omega$  is the frequency interval measured from the line center, and  $W(x)$  is the frequency interval at which the absorption coefficient has dropped to one half of its value at the line center.

The total intensity of the line is obtained by integrating Equation (1) over frequency. We can take the limits of integration to be  $\Delta\omega = -\infty$  and  $+\infty$ , since  $k(x)$  vanishes at large values of  $\Delta\omega$ , and we can take  $B(x, \omega)$  to be independent of  $\Delta\omega$  without introducing significant error, since  $B(x, \omega)$  is a slowly varying function of frequency.



The integral over frequency of the factors in Equation (1) that depend on  $\Delta\omega$  is then

$$I = \int_{-\infty}^{\infty} \frac{k_o W d\omega}{\pi (W^2 + \Delta\omega^2)} \exp \left\{ - \int_{x'}^x \frac{k_o W dx''}{\pi (W^2 + \Delta\omega^2)} \right\} \quad (4)$$

Making the substitution

$$y^2 = \frac{1}{\pi \Delta\omega^2} \int_{x'}^x k_o W dx'' \quad (5)$$

and recognizing that  $W^2$  is negligible in comparison with  $\Delta\omega^2$  over nearly all of the range of values of  $\Delta\omega$  that contribute significantly to the integral, we obtain

$$I = \int_{-\infty}^{\infty} \frac{k_o W e^{-y^2} dy}{\pi^{1/2} (u-u')^{1/2}} = \frac{k_o W}{(u-u')^{1/2}} \quad (6)$$

where we have introduced an effective optical thickness  $u(x)$ , defined by

$$u(x) = \int_{-R}^x k_o(x'') W(x'') dx'' \quad (7)$$

Equation (1), integrated over frequency, now becomes

$$I_+(x) = \int_{-R}^x k_o(x') W(x') B(x') \frac{dx'}{(u-u')^{1/2}} \quad (8)$$

Subtracting the similar expression for  $I_-(x)$ , the intensity of a beam travelling in the negative  $x$  direction, gives the following expression for the net flux in the  $x$  direction,  $\Gamma(x)$ .



$$-1/2 \Gamma(x) = \int_{-R}^R B(x') \frac{d|u-u'|^{1/2}}{dx'} dx' \quad (9)$$

where  $R$  is the boundary of the plasma in the positive  $x$  direction.

In order to perform the integration in Equation (9) it is necessary that  $B(x)$  and  $u(x)$  be known functions of  $x$ . For a plasma in local thermodynamic equilibrium, this requires that the temperature be a known function of  $x$ . If we set

$$y = x/R \quad (10)$$

and

$$v(y) = \int_0^y k_0(y'') W(y'') dy'' \quad (11)$$

then

$$u(x) = Rv(y) \quad (12)$$

and

$$\Gamma(x) = -2R^{1/2} \int_{-1}^1 B(y') \frac{d|v-v'|^{1/2}}{dy'} dy' \quad (13)$$

This means that the radiative flux is proportional to  $R^{1/2}$  if  $R$  is varied while keeping the temperature distribution (as a function of the normalized distance  $y$ ) unchanged.

We now have to calculate  $v(y)$  from Equation (11). The integrated absorption coefficient,  $k_0$ , is equal to

$$k_0 = \frac{2\pi^2 e^2 n_m f_{mn}}{mc} \quad (14)$$

where  $e$  is the electron charge,  $m$  is the electron mass,  $n_m$  is the concentration of atoms in the lower level of the line under consideration,  $f_{mn}$  is the absorption oscillator strength, and  $c$  is the velocity of light. For resonance lines under conditions where resonance broadening is the dominant



factor determining line width,

$$W = \frac{3\pi e^2 n_m f_{mn} g_m^{1/2}}{m\omega g_n^{1/2}} \quad (15)$$

where  $g_m$  and  $g_n$  are the statistical weights of the lower and upper states and  $\omega$  is the angular frequency at the line center. Thus  $k_{ow}$  is proportional to  $n_m^2$ , or approximately proportional to  $p^2/T^2$  if the temperature is not too high. Then

$$v(y) = \alpha \int_0^y \frac{dy}{\{T(y)\}^2} \quad (16)$$

where  $\alpha$  is a constant of proportionality incorporating the pressure and the atomic constants in Equations (14) and (15).

We now assume that the temperature distribution is parabolic, i.e.,

$$T(y) = T_0 (1 - by^2) \quad (17)$$

This form of distribution has been found to represent the actual temperature distribution reasonably well for arcs dominated by resonance radiation<sup>(2) (3)</sup>. With this distribution,  $v(y)$  is given approximately by

$$v(y) = \frac{\alpha y}{2 T_0} \left( \frac{1}{T_0} + \frac{1}{T(y)} \right) \quad (18)$$

A numerical calculation using Equations (17) and (18), with  $T_0 = 4000^\circ\text{C}$ ,  $T(1) = 1000^\circ\text{C}$  (typical values for a potassium arc) indicates that  $B(y)$  for resonance lines in a plasma with a parabolic temperature distribution can be represented quite closely by the equation

$$B(y) = B(0)e^{-a|v(y)|} \quad (19)$$

where  $a$  is a constant,



except for a small region near the origin where  $e^{-a|v|}$  has a discontinuous first derivative, while  $B(y)$  cannot have such a discontinuity. This is of little importance for the subsequent calculations, however. Using Equation (19), the integration in Equation (13) can be carried out to give, for the flux at the wall,

$$(R) = R^{1/2} \left\{ k_o(0) W(0) \right\}^{1/2} \left\{ 1 + \frac{T_o}{T(1)} \right\}^{1/2} \left\{ \frac{B(0)}{B(1)} \right\}^2 \quad (20)$$

to a good approximation.

Equation (20) must be integrated over solid angle to obtain the total flux in the line under consideration at the plasma boundary. In slab geometry this introduces a factor equal to

$$2\pi \int_0^{\pi/2} \cos^{1/2} \theta \sin \theta d\theta = \frac{4}{3} \pi \quad (21)$$

while in a cylindrically symmetrical plasma the additional factor is approximately

$$4 \int_0^{\pi/2} \sin^{3/2} \theta d\theta \int_0^{\pi/2} \cos^{9/2} \phi d\phi = 1.95 \quad (22)$$

and the total flux at the boundary of a cylindrical plasma is approximately

$$F(R) = 1.95 R^{1/2} \left\{ k_o(0) W(0) \right\}^{1/2} \left\{ 1 + \frac{T_o}{T(1)} \right\}^{1/2} \left\{ \frac{B(0)}{B(1)} \right\}^2 \quad (23)$$

For non-resonance lines, the theory presented here is applicable as far as Equation (14). The width of non-resonance lines in arc plasma is usually determined by Stark broadening, and is proportional to  $n_e$ , the electron concentration. The quantity  $k_o W$  is therefore proportional to  $n m n_e$ , or approximately proportional to  $\exp \left\{ \frac{-(E_m + E_i)}{kT} \right\}$  where  $E_m$  is the excitation potential for the



lower state of the line and  $E_i$  is the ionization potential. Therefore  $k_0 w$  effectively vanishes at some value  $y_1$  of the normalized radius. We can obtain a rough approximation for the flux in the non-resonance line at  $y_1$  by assuming a linear variation of  $k_0 w$  between the origin and  $y_1$ , and integrating Equation (13) with a constant value of  $B(y')$  equal to its axial value, since  $B(y_1)$  is not much smaller than  $B(0)$ . This is equivalent to saying that the emission in the line is confined to a region of nearly constant temperature near the axis. These approximations give

$$F(r_1) = 3.9 (R y_1)^{1/2} B(0) \left\{ k_0(0) w(0) \right\}^{1/2} \quad (24)$$

for the flux at  $r_1$ . The flux in the non-resonance line at the plasma boundary is smaller than this by the factor  $y_1$  ( $=r_1/R$ ) in cylindrical geometry, and is

$$F(R) = 3.9 R^{1/2} y_1^{3/2} B(0) \left\{ k_0(0) w(0) \right\}^{1/2} \quad (25)$$

It should be noted that, for non-resonance lines as well as for resonance lines, the flux at the wall is proportional to  $R^{1/2}$  if  $R$  is changed while keeping the temperature distribution unchanged.



LIST OF REFERENCES

1. E. A. Milne, "Thermodynamics of the Stars", in Handbuch der Astrophysik, v.3, part 1, 1930, pp 65-255, Equation (13), p. 103.
2. S. C. Brown, "Basic Data of Plasma Physics", Wiley, New York, 1959, p. 320.
3. T. S. Jen, M. F. Hoyaux and I. S. Frost, J. Quant. Spectrosoc. Radiat. Transfer, 9, 487 (1969).